Available online at www.sciencedirect.com
SCIENCE DIRECT
Lithos 89 (2006) 447–477
LITHOS
www.elsevier.com/locate/lithos

Mesoproterozoic rift-related alkaline magmatism at Elchuru, Prakasam Alkaline Province, SE India

D. Upadhyay [a,b,*], M.M. Raith [a], K. Mezger [b], K. Hammerschmidt [c]

[a] Mineralogisch-Petrologisches Institut, Poppelsdorfer Schloss, Universität Bonn, D-53115 Bonn, Germany
[b] Zentrallabor für Geochronologie, Mineralogisches Institut, Universität Münster, Corrensstrasse 24, D-48149 Münster, Germany
[c] Institut für Geologische Wissenschaften, FR Geochemie, Freie Universität, Malteserstraße 74-100, D-12249 Berlin, Germany

Received 11 May 2005; accepted 27 December 2005
Available online 10 March 2006

Abstract

The Elchuru alkaline complex in the Prakasam igneous province represents one occurrence of several alkaline bodies within the craton–Eastern Ghats Belt contact zone in Peninsular India. Nepheline syenites and associated mafic rocks intruded the cratonic crust at ≈1321 Ma and were deformed–metamorphosed to amphibolite facies condition during Pan-African times. Trace element compositions and Sr, Nd and Pb isotopic systematics indicate that the alkaline magma was derived from an enriched mantle source in the sub-continental lithosphere. The adjacent crusts of the Eastern Dharwar craton and the Eastern Ghats Belt were not involved either as source or as contaminants. The enriched mantle source was at least 1.9–2.1 Ga old as seen from the depleted mantle model ages of the rocks. The primary parent magma was a basanitic liquid that fractionated ferrokaersutite and clinopyroxene in the mantle, lowering the density sufficiently for the residual melt to intrude the crust. Magmatic differentiation in the suite can be explained by a two stage fractional crystallization model involving the removal of amphibole, clinopyroxene, allanite, titanite, apatite and zircon. The rift-related intra-continental setting of the complex indicates that alkaline magmatism represents the manifestation of a Mesoproterozoic continental breakup. Rifting along the cratonic margin may have led to the formation of several cratogenic basins (e.g., Chattisgarh basin, Indravati basin etc.) where stable shelf-type sediments could have been deposited on the passive margin during the Proterozoic. It could also have opened an ocean where some of the sediments of the Eastern Ghats Province may have been deposited.

Keywords: Alkaline-magmatism; Craton–Eastern Ghats Belt suture; Peninsular India; Continental rifting; Enriched mantle

1. Introduction

Alkaline rocks though volumetrically insignificant have incited a keen interest among petrologists all over the world because of their peculiar chemical compositions and exotic mineralogy, their specific tectonic associations and problems inherent in their petrogenesis. They can occur in all settings except at mid-oceanic ridges (Zhao et al., 1995) and their genesis has been explained by a number petrogenetic models. It has been suggested that alkaline magmas can form by partial melting of a metasomatised-mantle enriched in LREE and LILE (Dawson, 1987; Edgar, 1987). Others like Fitton (1987) have postulated low-degree partial melting

* Corresponding author. Present address: Zentrallabor für Geochronologie, Institut für Mineralogie, Universität Münster, Corrensstrasse 24, D-48149 Münster, Germany. Tel.: +49 251 8336107; fax: +49 251 8338397.
E-mail addresses: dewa_u@yahoo.co.in, upadhyay@uni-muenster.de (D. Upadhyay).

0024-4937/$ - see front matter © 2006 Elsevier B.V. All rights reserved.
doi:10.1016/j.lithos.2005.12.015

of an asthenospheric mantle with subsequent crystal fractionation for the formation of alkaline melts. Menzies (1987) on the other hand argues that alkaline magmas could be generated by the interaction of an asthenospheric melt with the lithospheric mantle.

In continental settings, nepheline syenite complexes are typically confined to well defined rift-related petrographic provinces (Platt, 1996). The formation of syenite and nepheline syenite in such settings has been attributed to two contrasting models: (i) crystal fractionation of nephelinite or alkali basalt magma (Bowen, 1928; Baker, 1987), (ii) low degree partial melting of mantle and/or crustal rocks (Bailey and Schairer, 1966; Bailey, 1974; Price et al., 1985).

In south-eastern India, the contact zone between the Bhandara/Eastern Dharwar cratons (EDC) and the Eastern Ghats Belt (EGB) contains several alkaline intrusives of rift-related geochemical affinity (Upadhyay et al., in press; Upadhyay and Raith, in press; present study; Upadyhyay and Raith, submitted for publication) which may mark the remnants of a paleo-rift at the eastern margin of the Indian shield (Fig. 1, inset). The crustal geodynamics during and subsequent to the rifting episode is important for understanding the Proterozoic evolution of the Indian subcontinent and may be crucial in any reconstruction of continental assembly.

This contribution presents the results of a detailed mineralogical, geochemical and geochronological study on rocks from the Elchuru nepheline syenite complex which represents one such occurrence at the craton–EGB contact (Fig. 1). The aim of the study is to constrain the time of emplacement and subsequent metamorphism of the alkaline rocks, to reconstruct their petrogenetic evolution by a synthesis of field, petrographic, geochemical and geochronological data and to

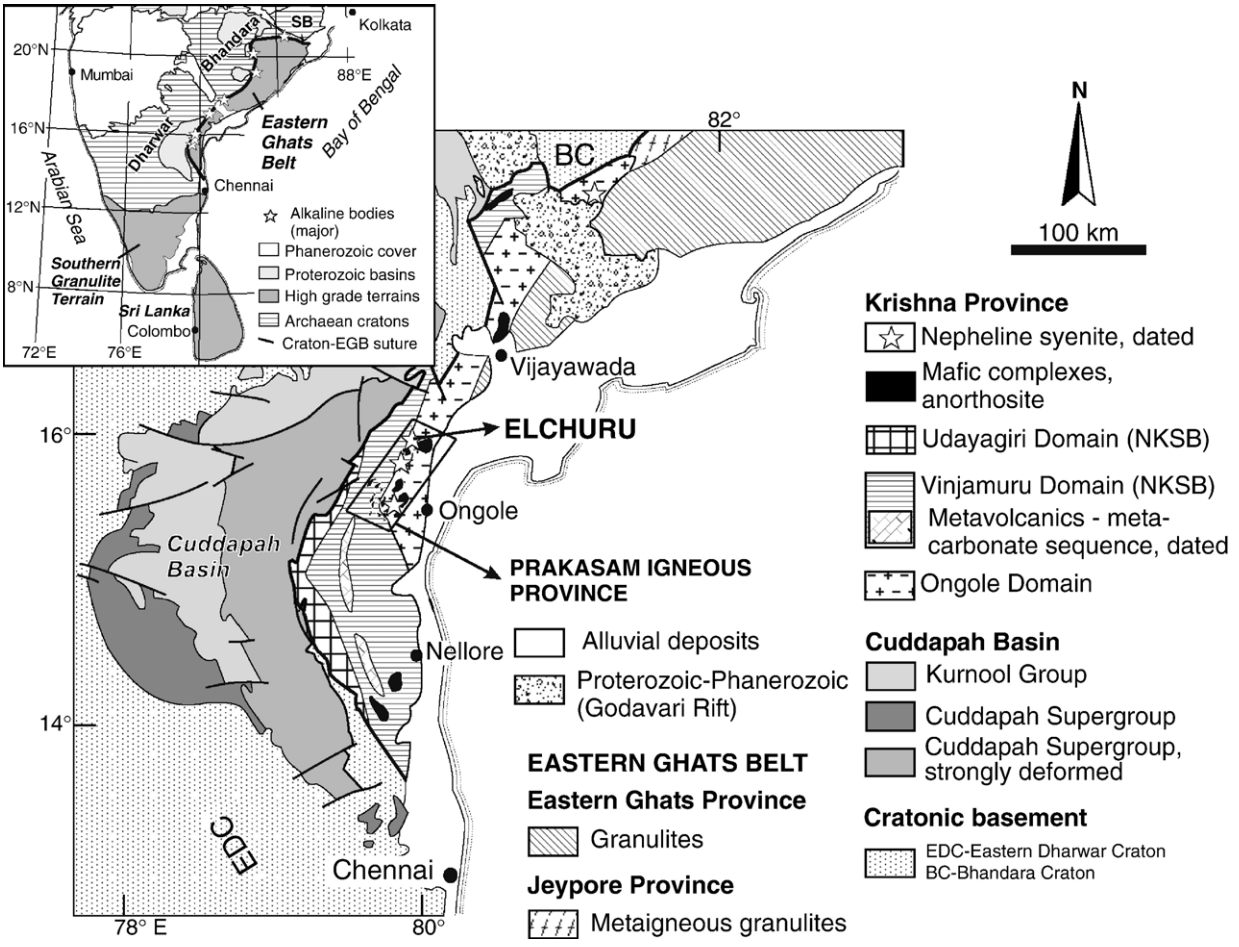

Fig. 1. Geology of the Krishna Province of the Eastern Ghats Belt (EGB) and surrounding regions showing the location of the Prakasam igneous province and the Elchuru alkaline complex (NKSB = Nellore Khammam Schist Belt). The inset shows a map of peninsular India with the locations of the major alkaline bodies along the craton–EGB contact zone (modified from Dobmeier and Raith, 2003).

deduce the broader geodynamic setting and resulting continental framework of the region during the Proterozoic.

2. Geologic setting and field relations

The craton–EGB contact in south-eastern India has been interpreted as a crustal suture related to Indo-Antarctic collisional events (Chetty and Murthy, 1994; Gupta et al., 2000; Bhadra et al., 2004) which resulted in the formation of the Proterozoic EGB orogen (Grew and Manton, 1986; Mezger and Cosca, 1999; Dasgupta and Sengupta, 2003; Dobmeier and Raith, 2003). The idea is supported by seismic and gravity anomalies which led Singh and Mishra (2002) to interpret the terrane boundary and associated shear zones along the eastern margin of the Dharwar craton to represent a cryptic collision suture between the EGB and the Cuddapah basin of the EDC (Fig. 1).

The EGB constitutes a poly-deformed and poly-metamorphosed orogen dominated by granulite facies migmatitic paragneisses that host intrusives of charnockites, enderbites, massif anorthosites, megacrystic granitoids and alkaline rocks. On the basis of recent isotopic data, Dobmeier and Raith (2003) have subdivided the belt and its contiguous terranes into a number of 'provinces' and 'domains' having contrasting evolutionary histories. South of the Godavari–Pranhita graben, the Ongole domain (erstwhile Western Charnockite Zone, WCZ) and the Udayagiri–Vinjamuru domains (erstwhile Nellore–Khammam-Schist-Belt, NKSB) form the composite lithotectonic association of the Krishna Province (Dobmeier and Raith, 2003) (Fig. 1).

The Elchuru alkaline complex is a part of the Prakasam igneous province defined by Proterozoic intrusives of granitoids, Si-undersaturated alkaline rocks, tholeiitic gabbros, rare carbonatites and lamprophyres (Leelanandam, 1980, 1981, 1989; Rao et al., 1987; Vijaya Kumar and Ratnakar, 1995; Sarkar and Paul, 1998) hosted in crystalline 'basement' rocks of probable cratonic affinity. Leelanandam (1989) suggested that the Prakasam province lies near the contact zone between charnockitic and non-charnockitic terrane which corresponds to the eastern margin of the 'non-charnockitic' Vinjamuru domain (NKSB) juxtaposed against the 'charnockitic' Ongole Domain (WCZ) (Fig. 1).

Dobmeier and Raith (2003) argue for a common geological history of the Ongole (WCZ) and the Udaigiri–Vinjamuru (NKSB) domains of the Krishna Province on the basis of similarity in isotopic age data for magmatism and metamorphism in the two adjoining terranes. The major tectonothermal event in the region occurred at ~1.65–1.55 Ga (Mezger and Cosca, 1999; Simmat, 2003) and postdates felsic magmatism at 1.87–1.77 Ga (Kovach et al., 2001; Vasudevan et al., in press). The alkaline magmatism in the Prakasam province appears to have a prolonged history between ~1370 and 1100 Ma (Sarkar and Paul, 1998) and thus postdates the 1.65–1.55 Ga tectonothermal event. However, field and microtextural evidence of deformation and the presence of a metamorphic foliation in the alkaline rocks indicate that they were affected by a later tectonothermal event (cf. Czygan and Goldenberg, 1989). Chalapathi Rao et al. (1996, 2004) have dated several kimberlites and lamproites from the EDC and the Cuddapah basin obtaining ages ranging from 1400 to 1090 Ma which is broadly coeval with alkaline magmatism in the Prakasam province. It is possible that they were the manifestation of the same tensional event that lead to the emplacement of alkaline and tholeiitic plutons in the Prakasam province. If this is correct, the basement hosting the Prakasam intrusives had already been amalgamated with the EDC by this time.

The poorly-exposed crystalline basement is dominated by granitic gneisses and amphibolites. Rao et al. (1987) infer four major episodes of folding in the host gneisses with the alkaline and gabbroic intrusions being emplaced during the waning phase of F_3 folding corresponding to D_3 deformation, giving rise to NNE–SSW trending outcrop patterns of the alkaline and other plutons concordant with the axis of the F_3 folding.

The Elchuru alkaline body lies in the northern part of the Prakasam province. It is inferred to be oval and exposed over an area of about 16 km^2 with its long axis parallel to the NE–SW 'trend of the province' (Madhavan and Leelanandam, 1988) (Fig. 2). The rocks are 'conformably enveloped' by gneisses with intercalations of black streaky amphibolites (Leelanandam, 1989). The complex is dominated by leucocratic nepheline syenite and subordinate mafic varieties which include ijolite, malignite, shonkinite, melanocratic nepheline diorite and mesocratic nepheline syenite (Czygan and Goldenberg, 1989; Ratnakar and Vijaya Kumar, 1995). The melanocratic members are confined to the central part of the complex where they occur as elongate lenses up to several tens of meters long in mesocratic to leucocratic nepheline syenite. At places the mafic rocks are intruded by veins and apophyses of nepheline syenite on centimeter scale. Late lamprophyre dyke swarms with sharp contacts cut across all lithologies in the alkaline complex. These dykes are steeply dipping; some assume lensoidal shape due to pinch and swell, and are confined

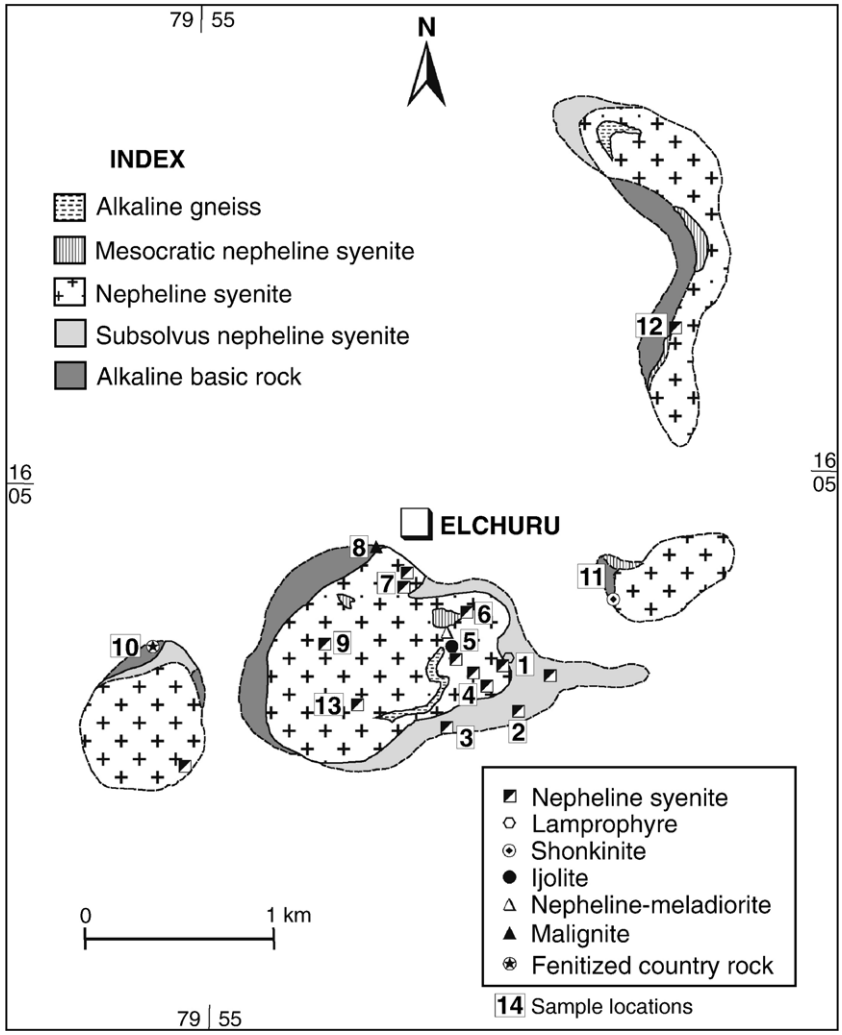

Fig. 2. Geological map of the exposed parts of the Elchuru alkaline complex (after Nag, 1983) showing the locations of the studied samples.

to the pluton (Madhavan et al., 1992). Angular and sub-angular fragments of nepheline syenite are found within the lamprophyre dykes at few places. The dykes themselves are intruded by nepheline–feldspar veins (Madhavan et al., 1992).

The leucocratic nepheline syenite appears homogeneous and massive in the central regions while it is deformed and shows an intense foliation towards the periphery of the complex. Madhavan and Leelanandam (1979) suggested that the gneissosity in the peripheral nepheline syenite had formed by an auto-metamorphic process during the emplacement of the alkaline body. Czygan and Goldenberg (1989) on the other hand, emphasize that foliation is developed in all parts of the alkaline complex and is the result of a regional metamorphic overprint.

3. Analytical technique

Major element abundances were analyzed at the Mineralogisch–Petrologisches Institut, University of Bonn, by X-ray fluorescence spectrometry on fused discs with a Philips PW-1480 X-ray spectrometer. For some samples, the rare earth elements (REE), Y and Sc concentrations were measured using ICP-AES (VARIAN, Vista MPX axial) while the other trace elements were analyzed by ICP-MS (VG-Plasma Quad PQ2+) at Geoforschungszentrum (GFZ), Potsdam. Details of the analytical technique are given in Zuleger and Erzinger (1988). The external reproducibility of the measured concentrations is better than 10% for most elements. Mineral compositions were determined at the Mineralogisch–

Petrologisches Institut, University of Bonn, using a WDS Cameca Camebax Microbeam electronprobe operating at an accelerating voltage of 15 kV and a beam current of 15 nA.

Whole rock Sm–Nd and Rb–Sr isotopic ratios were measured on a Finnigan MAT multicollector thermal ionization mass spectrometer at the Institut für Geologische Wissenschaften, Freie Universität, Berlin. Repeated analyses of NBS 987 Sr and La Jolla Nd standard yielded mean values of 0.710386±0.01% (2σ, 9 analyses) and 0.511822±0.007% (2σ, 9 analyses) for the $^{87}Sr/^{86}Sr$ and $^{143}Nd/^{144}Nd$ ratios, respectively. The isotope ratios given in Table 4 were corrected to accommodate the difference between the measured and recommended values for the NBS 987 Sr (0.71024) and La Jolla Nd (0.511858) standards (Lugmair et al., 1983). Pb isotopic ratios of leached feldspar separates were determined at the Zentrallaboratorium für Geochronologie, University of Münster, on a VG sector 54 mass spectrometer fitted with nine Faraday cups. Seven analyses of the NBS 982 Pb standard gave mean values of 0.027289±0.10% ($^{204}Pb/^{206}Pb$), 0.466665±0.057% ($^{207}Pb/^{206}Pb$) and 0.998623±0.11% ($^{208}Pb/^{206}Pb$) at the 2σ level for the isotopic ratios which yielded a mass discrimination factor of 0.08% per amu.

Zircons from a nepheline syenite sample were dated using the SHRIMP-II ion microprobe at the Centre for Isotopic Research, St. Petersburg, Russia. Details of the analytical technique can be found in Williams (1998). The error on the calibration of the standard was 0.54% for the U/Pb ratios. The data was reduced in a manner similar to that described by Williams (1998) using the SQUID Excel Macro of Ludwig (2000). The Pb/U ratios were normalized relative to a value of 0.0668 for the $^{206}Pb/^{238}U$ ratio of the TEMORA reference zircon, equivalent to an age of 416.75 Ma (Black and Kamo, 2003). The uncertainties given for the individual analysis (ratios and ages) are at the 1σ level but the uncertainties in calculated concordia ages are reported at 2σ levels (Table 2, Fig. 5). The Ahrens-Wetherill (1956) concordia plot was prepared using ISOPLOT/EX (Ludwig, 1999).

4. Petrography and mineral chemistry

4.1. Petrography

On the basis of field relations and petrography the alkaline rocks of the complex can be divided into mafic and felsic varieties. Details of the petrographic relations in these rock types are presented below.

4.1.1. Ijolite

This is a dark colored recrystallised rock consisting of nepheline, clinopyroxene and amphibole meeting at triple junctions. Amphibole is seen to replace clinopyroxene. Some partially recrystallised amphibole and clinopyroxene megacrysts can also be identified. Recrystallised titanite grains are abundant and often included in amphibole. Clinopyroxene and amphibole show sieve-like intergrowths with nepheline.

4.1.2. Shonkinite

This dark colored rock is porphyritic with megacrysts of clinopyroxene, some of which show oscillatory zoning. The groundmass consists of finer grained plagioclase, nepheline, biotite and clinopyroxene. Clinopyroxene megacrysts show replacement by a brownish amphibole and biotite along grain boundaries, cleavage planes and along the concentric zones seen in some grains. Accessory phases include minor titanite, sulfides (pyrhotite+chalcopyrite+pentlandite) and abundant apatite. The rock has a weak foliation defined by aligned biotite crystals in the groundmass. Textural relations suggest that some apatite may be cumulus crystals.

4.1.3. Melanocratic nepheline diorite

The rock is dominated by megacrysts of clinopyroxene, plagioclase and biotite. Plagioclase grains show replacement by nepheline giving rise to a 'myrmekite'-like intergrowth. The rock has a high modal abundance of apatite crystals. Opaque phases include pyrrhotite partially altered to hematite, chalcopyrite and large granular grains of ilmenite at the rims of femic phases. Biotite occurs as a primary igneous phase and also replaces opaque minerals and clinopyroxene. Some grains are strained showing undulose extinction and bent cleavage.

4.1.4. Malignite

This rock lacks any oriented fabric and is characterized by clusters of clinopyroxene and titanite showing partial to complete replacement by amphibole and biotite. The leucocratic 'groundmass' consists of recrystallised alkali feldspar and nepheline. A noteworthy feature is the high abundance of titanite and apatite some of which may be cumulus crystals. Opaque phases include minor pyrite and chalcopyrite.

4.1.5. Lamprophyre

It occurs as dykes with sharp contacts and finer-grained chilled margins. The grain size increases towards the central region of the dykes where the fabric is porphyritic. The phenocryst phases consist of euhedral to subhedral clinopyroxene and plagioclase.

Table 1
Representative microprobe analyses of minerals from Elchuru alkaline rocks

	Amphibole*									Biotite			
Rock type	Shonkinite	Malignite	Ne-syenite	Ne-syenite	Ne-syenite	Ijolite	Ne-syenite	Ne-syenite	Ne-mel-dt	Malignite	Shonkinite	Ne-syenite	Ne-syenite
Sample no	905	899	913	904	904	893	901	887	894	899	905	913	896
	fpg	fpg	fpg	fks	fks	Taramite	Taramite	Taramite					
SiO_2	40.22	39.52	38.86	40.35	40.48	39.35	37.00	38.51	34.88	33.98	35.27	34.62	34.48
TiO_2	3.77	3.75	3.19	4.47	4.51	1.32	2.59	1.53	7.89	6.92	5.35	5.84	6.04
Al_2O_3	12.53	13.11	12.41	11.95	11.73	13.47	14.00	12.87	13.95	14.06	14.32	13.40	15.04
Cr_2O_3	0.00	0.00	0.00	0.00	0.03	0.02	0.01	0.02	0.02	0.01	0.01	0.04	0.01
FeO	18.03	19.75	23.74	17.81	17.59	21.14	24.27	27.42	19.64	22.13	20.39	26.21	22.48
MnO	0.29	0.37	0.50	0.32	0.47	0.36	0.68	0.73	0.11	0.26	0.31	0.50	0.45
MgO	8.36	6.58	4.51	8.23	8.05	6.48	4.11	2.73	9.36	8.46	10.4	6.24	7.64
CaO	10.02	9.65	9.80	9.43	9.33	8.80	8.70	7.75	0.02	0.03	0.02	0.02	0.01
Na_2O	2.88	2.94	2.89	2.81	2.81	3.33	3.43	3.75	0.28	0.19	0.18	0.15	0.19
K_2O	1.93	2.09	2.34	2.15	2.12	2.46	2.38	2.61	9.67	9.31	9.86	9.75	10.27
Total	98.03	97.76	98.23	97.52	97.12	96.74	97.17	97.92	95.82	95.35	96.11	96.77	96.61
O basis	23	23	23	23	23	23	23	23	11	11	11	11	11
Cations													
Si	6.12	6.09	6.10	6.17	6.21	6.11	5.83	6.07	2.68	2.66	2.71	2.72	2.67
Ti	0.43	0.44	0.38	0.51	0.52	0.15	0.31	0.18	0.46	0.41	0.31	0.35	0.35
Al	2.25	2.38	2.29	2.15	2.12	2.47	2.60	2.39	1.26	1.30	1.30	1.24	1.37
Cr^{+3}	0.00	0.00	0.00	0.00	0.00	0.00	0.00	0.00	0.00	0.00	0.00	0.00	0.00
Fe^{+3}	0.10	0.06	0.11	0.09	0.06	0.55	0.65	0.79	0.00	0.00	0.00	0.00	0.00
Fe^{+2}	2.19	2.49	3.00	2.18	2.20	2.20	2.55	2.83	1.26	1.45	1.31	1.73	1.46
Mn	0.04	0.05	0.07	0.04	0.06	0.05	0.09	0.10	0.01	0.02	0.02	0.03	0.03
Mg	1.90	1.51	1.05	1.87	1.84	1.50	0.97	0.64	1.07	0.99	1.19	0.73	0.88
Ca	1.63	1.59	1.65	1.54	1.53	1.46	1.47	1.31	0.00	0.00	0.00	0.00	0.00
Na	0.85	0.88	0.88	0.83	0.84	1.00	1.05	1.15	0.04	0.03	0.03	0.02	0.03
K	0.37	0.41	0.47	0.42	0.41	0.49	0.48	0.53	0.95	0.93	0.97	0.98	1.02

Abbreviations: fpg = ferropargasite, fks = ferrokaersutite, Ne-mel-dt = nepheline meladiorite, Lamp = lamprophyre, Ne-syenite = nepheline syenite.
*Ferric iron estimate and nomenclature of amphibole follows the scheme recommended by Leake et al. (1997). See Tables 3a, 3b and Fig. 2 for sample locations.

	Clinopyroxene*									Nepheline			
Rock type	Lamp	Ijolite	Ne-mel-dt	Malignite	Shonkinite	Ne-syenite	Ne-syenite	Ne-syenite	Ne-syenite	Malignite	Ne-mel-dt	Ne-syenite	Ne-syenite
Sample no	885	893	894	899	905	90	90	901	901	899	894	887	901
						Core	Rim	Core	Rim				
SiO_2	51.27	51.53	50.86	50.14	51.17	48.50	49.81	49.88	51.15	42.78	42.60	42.49	42.12
TiO_2	1.11	0.28	1.25	1.10	0.66	0.24	0.26	0.58	0.41	0.00	0.00	0.03	0.00
Al_2O_3	3.49	5.02	3.70	2.67	3.25	1.83	2.60	2.47	2.35	33.5	34.1	34.0	33.8
Cr_2O_3	0.26	0.02	0.00	0.00	0.00	0.04	0.00	0.00	0.03	0.00	0.00	0.00	0.00
FeO	9.38	13.55	10.01	13.52	11.12	21.24	21.01	18.68	17.67	0.04	0.09	0.08	0.07
MnO	0.18	0.28	0.21	0.37	0.39	0.88	0.88	0.80	0.67	0.00	0.01	0.01	0.04
MgO	10.81	7.06	10.56	8.80	10.60	4.00	3.75	5.49	6.22	0.00	0.00	0.01	0.04
CaO	20.92	16.02	21.55	20.81	20.44	20.50	17.44	19.88	18.05	0.53	0.68	0.20	0.57
Na_2O	1.84	4.60	1.64	1.46	1.56	1.55	3.57	2.22	3.33	16.36	17.33	16.92	17.54
K_2O	0.14	0.00	0.02	0.02	0.17	0.00	0.09	0.00	0.06	6.14	5.34	6.12	5.41
Total	99.42	98.36	99.80	98.88	99.36	98.78	99.40	100.0	99.94	99.31	100.2	99.86	99.54
O basis	6	6	6	6	6	6	6	6	6	32	32	32	32
Cations													
Si	1.92	1.95	1.91	1.93	1.93	1.93	1.94	1.93	1.95	8.29	8.18	8.20	8.16
Ti	0.03	0.01	0.04	0.03	0.02	0.01	0.01	0.02	0.01	0.00	0.00	0.00	0.00
Al	0.15	0.22	0.16	0.12	0.14	0.09	0.12	0.11	0.11	7.64	7.72	7.74	7.71
Cr^{+3}	0.01	0.00	0.00	0.00	0.00	0.00	0.00	0.00	0.00	0.00	0.00	0.00	0.00
Fe^{+3}	0.07	0.20	0.07	0.07	0.08	0.15	0.26	0.16	0.21	0.01	0.01	0.01	0.01
Fe^{+2}	0.22	0.23	0.24	0.37	0.27	0.56	0.43	0.45	0.35	0.00	0.00	0.00	0.00
Mn	0.01	0.01	0.01	0.01	0.01	0.03	0.03	0.03	0.02	0.00	0.00	0.00	0.01
Mg	0.60	0.40	0.59	0.50	0.60	0.24	0.22	0.32	0.35	0.00	0.00	0.00	0.01
Ca	0.84	0.65	0.86	0.86	0.83	0.88	0.73	0.82	0.74	0.11	0.14	0.04	0.12
Na	0.13	0.34	0.12	0.11	0.11	0.12	0.27	0.17	0.25	6.15	6.45	6.33	6.59
K	0.01	0.00	0.00	0.00	0.01	0.00	0.00	0.00	0.00	1.52	1.31	1.51	1.34

Abbreviations: Ne-mel-dt = nepheline meladiorite, Lamp = lamprophyre, Ne-syenite = nepheline syenite. *Ferric iron in clinopyroxene estimated using stoichiometric criteria based on 4 cations and 6 oxygens per formula unit. See Tables 3a,b and Fig. 2 for sample locations.

Clinopyroxene grains often show concentric oscillatory zoning and are replaced by brownish amphibole. Plagioclase phenocrysts are recrystallised to polygonal mosaics, but still preserve the lath like crystal shapes. The groundmass consists of fine-grained clinopyroxene, nepheline, plagioclase, biotite and minute grains of graphite and pyrite. The rock lacks any prominent oriented fabric.

4.1.6. Nepheline syenite

The nepheline syenite is a leucocratic medium to coarse grained rock often showing a foliation defined by oriented mafic minerals/clusters and deformed alkali feldspar and nepheline. Mafic phases include biotite, clinopyroxene and amphibole which often occur as clusters. Titanite, apatite, zircon, magnetite–ilmenite, rare allanite and calcite make up most of the accessory phases. Nepheline and alkali feldspar show replacement by cancrinite, calcite and natrolite. Alkali feldspar is micro- to crypto-perthite and the host K-feldspar is microcline. Biotite occurs as discrete crystals but also replaces clinopyroxene and amphibole. Clinopyroxene grains in some weakly deformed varieties show strong zonation. In others, they are recrystallised and replaced by amphibole. Opaque phases are minor and include magnetite with ilmenite and spinel exsolution lamellae/spindles, pyrrhotite, chalcopyrite and pyrite.

4.2. Mineral chemistry

Representative microprobe analyses of mineral compositions are listed in Table 1. Clinopyroxenes in most nepheline syenites are diopside–hedenbergite–aegirine augite solid solutions (Fig. 3). In the more mafic rocks, higher Al contents (up to 0.22 *apfu*) result in high Ca-Tschermakite and jadeite components (Fig. 3). The compositional trend shows an increase of Fe^{3+} with differentiation. Clinopyroxenes from the ijolite and some nepheline syenites have higher Na/(Na+Ca) ratios correlated with high Al^{VI} which can be explained by jadeite substitution during the metamorphic overprint. Similar, aluminous pyroxenes from the North Nyasa Alkaline Province of central and northern Malawi having high Al^{VI} have been interpreted by Woolley et al. (1996) to be of metamorphic origin. Compositional variation in biotites is characterized by a trend of increasing Fe^{2+}/Mg ratio (1–2.8) at constant Al content and is similar to the evolutionary trend of biotites from the Chilwa province nepheline syenites and the silica oversaturated felsic rocks in Malawi (Woolley and Platt, 1986). High TiO_2 contents (4.0–7.9 wt.%) of the biotites indicate fairly high temperatures of equilibration (Luhr et al., 1984; Schreurs, 1985). Amphiboles in the alkaline rocks belong to both the calcic and sodic–calcic groups (Fig. 4). The calcic group comprises titanium-rich ferropargasite and ferrokaersutite while the sodic–calcic group is dominated by the iron-rich amphibole taramite. Ferrokaersutite must have been a liquidus phase while taramite is the product of metamorphic/metasomatic alteration of pre-existing amphiboles as has been seen in the metamorphosed assemblage of the Mbozi alkaline complex, Tanzania (Mitchell, 1990). Nepheline compositions bracket the range $Ne_{77–83.1}Ks_{16.8–22.9}Qtz_{0–3.4}$ with up to 3.5% anorthite and <0.4% Fe-nepheline

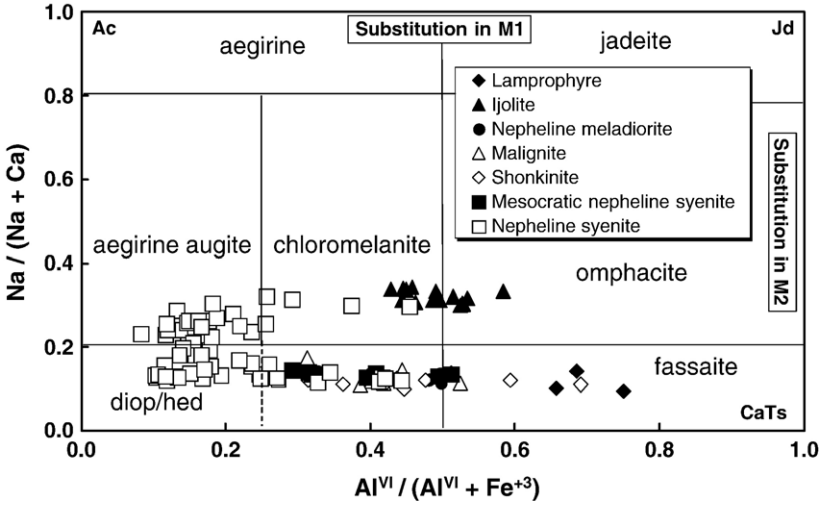

Fig. 3. Composition of clinopyroxenes from the Elchuru alkaline rocks showing the extent of aegirine–jadeite–Ca-Tschermakite solid solutions. The compositional trend shows an increase of Fe^{3+} with differentiation. Clinopyroxenes from the ijolite and some nepheline syenites have higher Na/(Na+Ca) ratios and high Al^{VI} which can be explained by jadeite substitution.

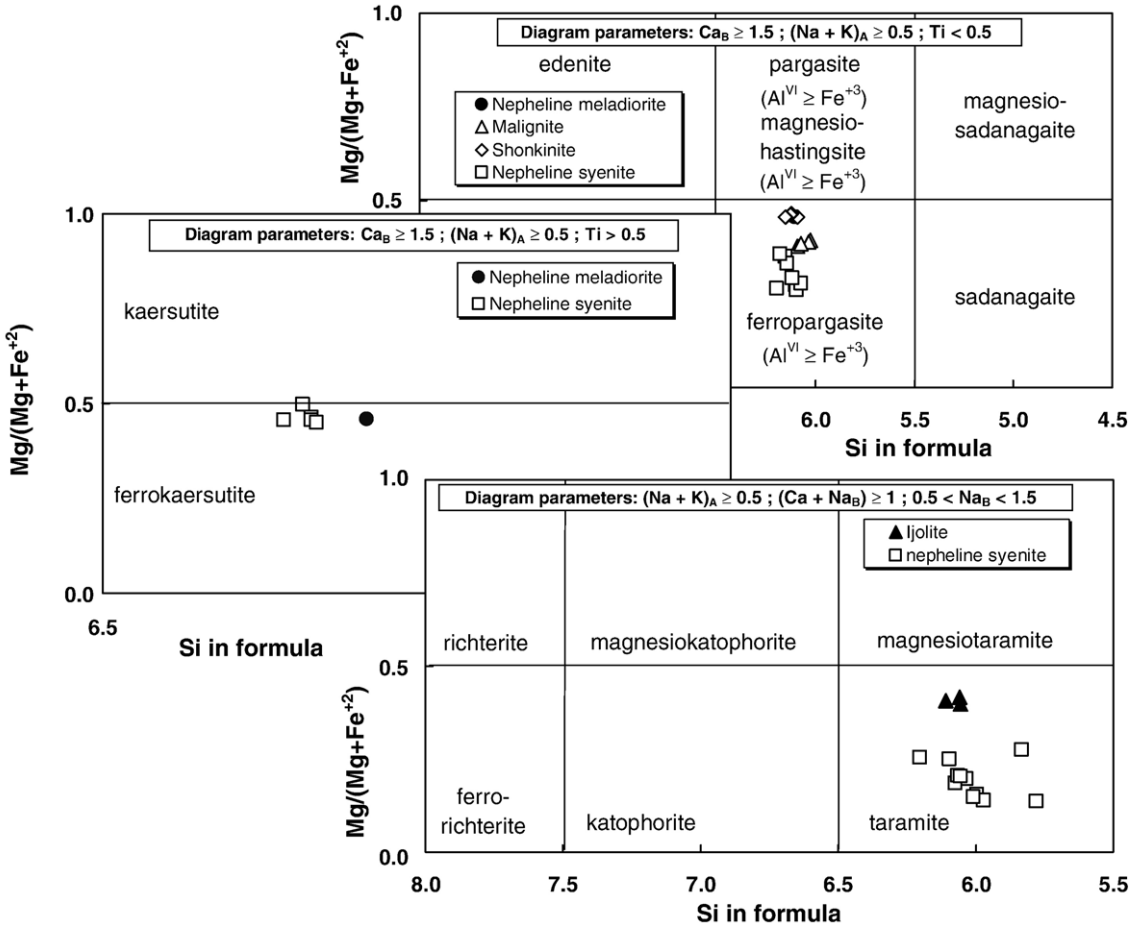

Fig. 4. Compositions of amphiboles from the Elchuru alkaline rocks. Both calcic and sodic–calcic groups can be recognized. The classification follows the recommendations of Leake et al. (1997).

components. The low silica solid solution suggests equilibration below 500 °C (Hamilton and Mackenzie, 1960) which must obviously correspond to post-metamorphic re-equilibration rather than magmatic cooling.

5. Intrusion age and age of metamorphism

Subba Rao et al. (1989) have obtained a whole rock Rb–Sr isochron age of 1242±33 Ma for the Elchuru alkaline rocks which they interpret to date magma emplacement. The Rb–Sr system however, may have been affected by post-magmatic events making the age unreliable. In this study, the age of magmatic crystallization is constrained by dating zircons from a nepheline syenite sample (No. 899) using the SHRIMP-II ion microprobe (Table 2). The cathodoluminescence (CL) images reveal complex internal structures of the crystals with evidence of recrystallisation and exsolution overprinting magmatic zoning (Fig. 5 inset). The U and Th concentrations are highly variable; nevertheless six out of the eight analyzed points define a concordia age of 1321±17 Ma (2σ) (Fig. 5). Together with the two discordant points, the data define a discordia with intercepts of 1308±31 and 721 ±210 Ma (2σ) (Fig. 5). A broadly coeval zircon upper intercept age of 1352±7 Ma has been obtained for the Uppalapadu nepheline syenite pluton to the south of Elchuru in the Prakasam province (Carol D. Frost, personal communication). The concordant age of 1321 ±17 Ma is hence interpreted to date the intrusion of the Elchuru alkaline rocks.

Field and petrographic evidences such as the presence of a metamorphic foliation and partial to complete recrystallisation of minerals support the findings of Czygan and Goldenberg (1989) that the alkaline rocks have been overprinted by a tectonothermal event. The mineral assemblages suggest that the metamorphism

Table 2
U–Th–Pb SHRIMP isotope data from zircons and Rb–Sr isotope data from biotite–whole rock pairs and their isochron ages

Spot	U (ppm)	Th (ppm)	^{206}Pbc (%)	^{206}Pb* (ppm)	^{232}Th/^{238}U	^{238}U/^{206}Pb (total)±%	^{207}Pb/^{206}Pb (total)±%	^{206}Pb/^{238}U age (Ma)[1]	^{208}Pb/^{232}Th age (Ma)[1]	^{207}Pb/^{206}Pb age (Ma)[1]	% disc.	^{207}Pb*/^{206}Pb*±%	^{207}Pb*/^{235}U±%	^{206}Pb*/^{238}U±%	Error corr.
899.1.1	225	134	–	43.7	0.62	4.42±1.4	0.0842±1.1	1316±17	1420±48	1297±21	−1	0.0842±1.1	2.63±1.8	0.227±1.4	0.79
899.2.1	230	114	0.20	43.5	0.51	4.54±1.3	0.0847±1.1	1282±15	1254±27	1269±28	−1	0.0830±1.4	2.52±1.9	0.220±1.3	0.67
899.2.2	797	1121	1.24	148	1.45	4.64±1.2	0.0948±1.2	1243±13	1575±120	1300±50	5	0.0843±2.6	2.47±2.8	0.213±1.2	0.42
899.2.3	49	116	–	9.58	2.46	4.38±1.6	0.0860±2.2	1328±20	1327±28	1359±43	2	0.0869±2.2	2.74±2.8	0.229±1.6	0.59
899.3.1	705	291	0.26	158	0.43	3.83±1.6	0.0882±1.5	1492±21	2105±44	1338±32	−10	0.0860±1.7	3.09±2.3	0.260±1.6	0.69
899.3.2	205	91	0.17	39.7	0.46	4.44±1.3	0.0852±1.1	1306±15	1309±30	1287±29	−1	0.0838±1.5	2.59±2.0	0.225±1.3	0.64
899.4.1	387	78	0.02	77.6	0.21	4.29±1.2	0.0857±0.9	1351±15	1393±25	1328±17	−2	0.0855±0.9	2.75±1.5	0.233±1.2	0.81
899.4.2	28	187	2.59	6.39	6.79	3.83±2.1	0.108±2.7	1462±30	1351±38	1339±200	−8	0.0861±10	3.02±11.0	0.255±2.3	0.22
899.4.3	485	842	–	97.2	1.80	4.28±1.2	0.0857±0.7	1353±14	1351±17	1338±14	−1	0.0860±0.7	2.77±1.4	0.234±1.2	0.86
899.5.1	448	664	0.63	67.7	1.53	5.68±1.2	0.0835±0.9	1039±12	1387±20	1153±33	11	0.0783±1.7	1.89±2.0	0.175±1.2	0.59

Sample	Rock type	Desc.	Rb (ppm)	Sr (ppm)	^{87}Rb/^{86}Sr	^{87}Sr/^{86}Sr	2σ mean	Age (Ma)
888	Ne-Syenite	biotite	607	7.620	275.9	2.72881	0.00019	
		W.R.	127	506.3	0.727	0.717806	0.000013	513±3
910	Ne-Syenite	biotite	575	21.70	81.28	1.31230	0.00005	
		W.R.	144	1570	0.265	0.708789	0.000019	523±2
895	Ne-Syenite	biotite	619	40.30	45.99	1.07091	0.00002	
		W.R.	140	2378	0.170	0.707165	0.000017	557±2

Pbc and Pb* indicate the common and radiogenic Pb, respectively; (1) Common lead corrected using measured ^{204}Pb. The errors on the isotopic ratios and the ages are reported at 1σ level. The abbreviations W.R. and Ne-syenite refer to whole rock and nepheline syenite, respectively.

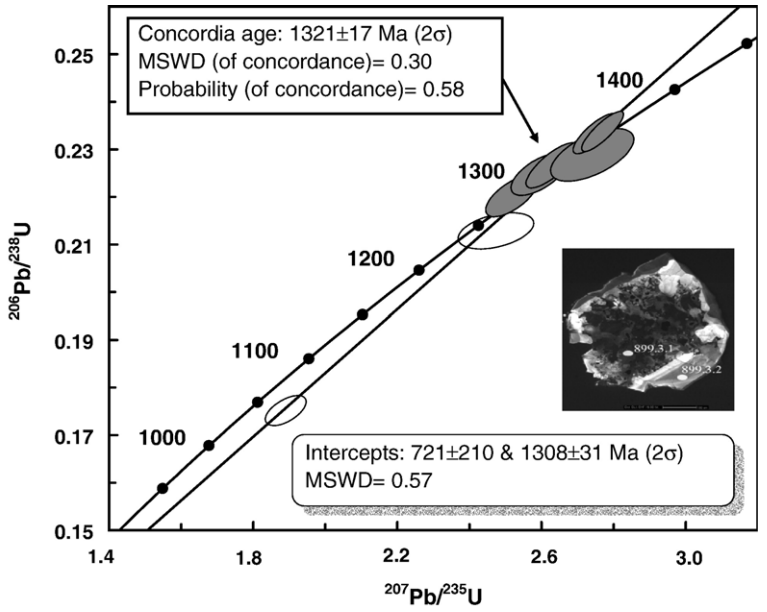

Fig. 5. U–Pb concordia diagram showing SHRIMP U–Th–Pb data from zircons of nepheline syenite sample 899. The data define a discordia with intercepts at 1308±31 (2σ) and 721±210 Ma (2σ). The concordant data points give a mean age of 1321±17 Ma (2σ) which is interpreted to date magmatic crystallization. The inset shows a CL image (with analytical spots) of one analyzed zircon grain. Recrystallisation textures can be seen to overprint igneous zoning.

reached amphibolite-facies condition. Rb–Sr isotopic ratios from three biotite–whole rock pairs give isochron ages ranging from 513±3 (2σ) to 557±2 Ma (2σ) which indicates the presence of a Pan-African thermal imprint (Table 2). Such an inference is supported by the recrystallisation textures seen in zircon CL images and the discordance of some analyses. The zircon lower concordia intercept (though not well constrained) lies within the cluster of Pan-African mineral ages reported for this region (443–676 Ma; reviewed in Sarkar and Paul, 1998). Pan-African ages between 611–484 Ma have also been obtained from amphibole (K–Ar), nepheline (K–Ar), apatite (U–Pb), biotite (Rb–Sr) and titanite (U–Pb) from the Khariar and Kunavaram alkaline complexes which indicates that the craton–EGB suture was tectonically active during the Pan-African orogeny (Aftalion et al., 2000; Upadhyay et al., in press; Upadyhyay and Raith, submitted for publication). The Pan-African biotite–whole rock ages from the Elchuru alkaline rocks are hence interpreted to date cooling following the Pan-African metamorphic overprint on the rocks.

6. Major and trace element characteristics

Representative major and selected trace element analyses for the rocks are listed in Table 3a and the REE analyses are given in Table 3b. The rocks have high alkali concentrations (Na_2O+K_2O=6–17 wt.%) and low SiO_2 (40–56 wt.%). The agpaitic index [$(Na_2O+K_2O)/Al_2O_3)_{molar}$] (0.7–1) mirrors the miaskitic mineralogy and the K_2O/Na_2O ratios (0.4–1.9) gives them sodic to mildly potassic affinities. The low abundances of compatible elements like Ni (0.4–143 ppm), Cr (15.5–396 ppm), Sc (0.3–21 ppm) and Co (1.4–45 ppm) suggest that most rocks represent evolved compositions, the large variations indicating dominance of fractional crystallization processes in their evolution. The abundances of large ion lithophile (LIL) elements like Rb (25–222 ppm), Sr (280–4768 ppm) and Ba (60–3381 ppm) and the high field strength (HFS) elements such as Zr (26–442 ppm), Hf (0.7–8.4 ppm), Nb (27–289 ppm) and Ta (1.1–11.2 ppm) also show a large variation in the suite. A strong enrichment is seen of the light rare earth elements (LREE) ($La_N \approx 69–648$).

The major element concentrations also show a large variation in the suite (Fig. 6). Al_2O_3 is chosen as a fractionation index in variation diagrams because (i) it is less susceptible to post-magmatic changes and shows a large variation in the suite (12–24 wt.%), (ii) extremely low MgO concentrations (Table 3a) make any Fe–Mg based index unreliable, (iii) use of SiO_2 as a differentiation index produces scatter in the trends which can be attributed to the presence of cumulus nepheline/alkali feldspar in some rocks. The major elements define good trends in which Na_2O, K_2O and

Table 3a
Representative major and selected trace element analyses of Elchuru alkaline rocks

Rock type	Lamp	Lamp	Ijolite	Ne-mel-dt.	Malignite	Shonkinite	Mes. Ne-syenite	Ne-syenite	Ne-syenite	Ne-syenite	Ne-syenite	Ne-syenite	Ne-syenite	Ne-syenite	Ne-syenite	Ne-syenite	Ne-syenite	Ne-syenite	Ne-syenite
Location	1	1	5	5	8	11	4	1	2	3	4	5	6	7	7	9	12	13	14
Sample no.	884	885	893	894	899	905	890	883	887	888	891	892	895	896	897/2	901	909	910	912
Major elements (wt.%)																			
SiO_2	45.72	46.65	42.58	40.59	43.31	46.08	44.95	55.17	56.01	54.02	54.36	53.35	53.32	53.47	52.93	55.46	53.03	52.68	54.01
TiO_2	1.86	2.20	2.71	4.28	3.26	2.23	2.27	0.36	0.26	0.35	0.35	0.76	0.79	0.35	0.35	0.17	0.35	0.69	0.36
Al_2O_3	16.15	13.71	15.84	12.08	15.50	14.39	14.29	22.58	22.23	22.29	21.60	21.52	21.54	22.35	20.24	23.91	20.30	21.33	21.68
Fe_2O_3*	12.37	10.65	13.73	15.98	12.87	12.17	11.19	2.90	3.52	4.39	5.34	3.92	5.00	4.86	8.44	1.09	8.44	5.47	4.71
MnO	0.17	0.14	0.26	0.20	0.19	0.19	0.21	0.06	0.08	0.10	0.13	0.07	0.11	0.09	0.18	0.02	0.18	0.10	0.10
MgO	6.04	7.89	4.40	6.85	4.25	6.67	7.37	0.44	0.30	0.43	0.33	0.79	0.96	0.45	0.65	0.17	0.64	0.66	0.44
CaO	8.67	8.19	11.18	10.79	8.42	8.62	8.52	1.53	1.48	1.88	1.72	2.33	2.72	1.69	2.71	0.76	2.71	2.05	2.22
Na_2O	4.60	3.80	5.93	3.04	3.87	4.07	3.54	7.11	6.46	7.24	6.22	5.18	6.41	7.55	6.59	8.22	6.60	6.70	6.81
K_2O	3.01	4.68	2.55	3.12	4.65	4.10	5.61	8.65	9.06	8.21	8.92	10.01	7.89	7.65	6.71	8.83	6.71	8.01	8.57
P_2O_5	0.42	0.58	0.81	1.79	1.45	0.77	0.69	0.10	0.09	0.12	0.10	0.20	0.33	0.17	0.35	0.09	0.35	0.23	0.16
SO_3	0.03	0.04	0.02	0.07	0.06	0.04	0.02	0.00	0.01	0.01	0.01	0.01	0.01	0.01	0.01	0.01	0.03	0.01	0.01
Total	99.29	98.97	100.2	99.36	98.84	99.79	99.15	99.07	99.63	99.16	99.22	98.72	99.52	98.82	99.43	98.97	99.58	98.23	99.34
CIPW norm (wt.%)																			
Plagioclase	21.1	6.9	9.3	10.6	11.8	11.5	6.8	14.1	15.9	12.8	12.5	6.1	16.0	15.9	22.5	11.1	23.0	13.2	9.6
Orthoclase	18.1	28.4	2.6	15.1	26.7	24.6	13.9	51.8	54.0	49.2	53.4	58.6	47.3	46.0	40.2	52.9	40.2	48.6	51.3
Nepheline	18.1	17.7	27.4	14.1	18.1	17.6	16.5	27.7	23.9	28.9	24.7	24.2	24.8	29.1	21.7	33.4	21.4	26.8	28.2
Leucite	0.0	0.0	10.0	3.0	1.4	0.0	15.7	0.0	0.0	0.0	0.0	1.5	0.0	0.0	0.0	0.0	0.0	0.0	0.0
Diopside	21.9	25.7	34.9	27.4	19.6	24.6	26.4	2.7	1.8	4.0	2.9	3.9	4.8	2.6	4.9	1.2	4.6	4.1	6.3
Olivine	14.3	14.2	6.7	14.8	10.9	13.8	11.4	2.0	2.8	2.9	4.0	2.6	3.5	3.8	6.7	0.6	6.8	3.9	2.3
Ilmenite	3.6	4.3	5.2	8.4	6.4	4.3	4.4	0.7	0.5	0.7	0.7	1.5	1.5	0.7	0.7	0.3	0.7	1.4	0.7
Magnetite	1.8	1.6	2.0	2.4	1.9	1.8	3.3	0.9	1.0	1.3	1.6	1.2	1.5	1.4	2.5	0.3	2.5	1.6	1.4
Apatite	1.0	1.4	1.9	4.3	3.5	1.8	1.6	0.2	0.2	0.3	0.2	0.5	0.8	0.4	0.8	0.2	0.8	0.6	0.4
Zircon	0.03	0.03	0.01	0.04	0.07	0.04	0.04	0.03	0.01	0.03	0.04	0.04	0.04	0.03	0.1	0.0	0.04	0.03	0.01
D.I.+	57.3	52.9	49.2	42.8	58.0	53.7	52.9	93.6	93.7	90.9	90.6	90.4	88.1	91.0	84.4	97.4	84.6	88.6	89.1
Trace elements (ppm)																			
Sc	20	19	23	21	9.5	20	18	1.03	0.67	0.64	0.92	1.31	1.60	0.87	2.77	0.26	2.58	1.40	0.52
V	130	160	199	182	33	164	159	4.2	3.3	2.1	3.2	8.3	7.5	3.1	23.3	2.1	0.7	8.3	3.6
Cr	47	396	99	118	16	264	331	57	59	49	58	46	44	45	78	51	39	34	49
Ni	46	143	25	61	2.2	70	104	4.1	2.2	3.4	2.6	4.1	0.62	0.39	8.2	6.8	0.63	4.5	2.8
Co	46	42	22	45	23	36	37	3.5	2.7	3.9	3.5	5.3	5.7	3.4	7.8	1.4	4.1	5.1	4.4
Cu	31	46	0.80	26	14.3	23	21	3.9	1.71	4.7	3.8	5.3	5.6	3.3	13	4.0	27	7.3	6.0
Zn	78	71	94	97	82	103	117	60	26	32	56	52	48	37	69	8.5	90	64	72
Cs	0.46	1.18	0.12	0.92	0.61	1.29	2.95	0.56	0.35	0.7	0.79	1.5	0.87	0.68	0.3	0.81	0.78	1.32	
Rb	53	120	25	83	58	105	189	135	169	138	222	220	140	168	214	124	217	144	187
Sr	613	947	486	1077	4768	1160	1012	775	582	507	492	3442	2378	821	280	1821	281	1570	1562
Ba	961	1744	416	2776	3381	1816	2019	248	353	168	348	1428	1163	278	77	291	60	543	437
Y	18	20	17	34	36	24	25	11	7.1	12	8.9	15	19	9.4	26	5.4	35	17	0.87
Zr	103	180	97	191	356	256	199	119	92	149	189	187	187	137	442	26	237	131	58
Hf	2.71	5.06	2.54	5.63	8.37	5.65	5.30	3.28	2.92	4.22	4.58	5.26	4.86	3.79	10.92	0.65	6.91	3.84	1.83
Nb	26.7	67.7	40.3	52.4	143	72.0	99.3	93.3	80.4	124	160	79.2	117	114	260	26.8	289	160	133
Ta	1.54	4.05	1.10	3.24	8.41	4.00	4.99	4.59	3.58	5.10	5.14	3.99	6.25	6.7	9.78	2.42	11.17	7.47	5.67
Th	3.38	5.13	2.68	6.86	6.26	7.22	15.60	4.22	1.42	3.03	2.00	8.78	6.83	3.68	6.66	6.15	12.00	10.8	6.14
U	0.74	1.08	0.87	1.22	1.31	1.65	2.15	0.75	0.20	0.44	0.24	0.93	1.29	0.64	0.92	1.68	2.04	1.42	0.93
Pb	6.01	8.86	4.57	14.9	10.0	17.0	7.09	12.4	6.55	10.5	6.23	14.4	15.5	9.77	14.9	15.3	21.4	16.5	9.83

Abbreviations used are the same as in Table 1; The locations of the samples are shown in Fig. 2; *Total iron as Fe_2O_3; + differentiation index after Thornton and Tuttle (1969).

Table 3b
Representative REE analyses of Elchuru alkaline rocks

Rock	Lamp	Lamp	Ijolite	Ne-mel-dt.	Malignite	Shonkinite	Mes. Ne-syenite	Ne-syenite	Ne-syenite	Ne-syenite	Ne-syenite	Ne-syenite	Ne-syenite	Ne-syenite	Ne-syenite	Ne-syenite	Ne-syenite	Ne-syenite	Ne-syenite
Location	1	1	5	5	8	11	4	1	2	3	4	5	6	7	7	9	12	13	14
Sample	884	885	893	894	899	905	890	883	887	888	891	892	895	896	897/2	901	909	910	912
La	32.0	60.0	31.8	120	212	76.7	118	60.0	40.7	69.0	45.2	84.0	79.8	45.2	165	25.4	238	83.0	58.1
Ce	62.0	116	66.5	239	339	140	207	108	83.8	132	91.5	142	153	93.1	264	55.5	366	159	113
Pr	6.49	13.0	8.04	23.5	29.7	15.5	18.3	11.0	8.92	11.7	9.56	15.0	16.7	9.83	23.2	4.95	31.0	17.0	12.5
Nd	24.9	43.3	31.5	83.4	109	56.4	58.8	29.8	29.2	37.5	31.2	47.6	58.4	32.0	78.1	17.0	103	52.0	39.6
Sm	4.45	6.98	5.49	14.1	16.4	8.95	8.50	3.91	4.10	5.01	4.28	6.78	8.99	4.53	11.8	2.62	13.1	8.90	5.51
Eu	1.90	2.30	2.36	4.20	5.43	2.73	2.70	1.50	1.07	1.60	1.07	3.01	3.35	1.38	3.03	1.57	2.17	2.60	1.87
Gd	4.70	6.40	5.02	13.0	13.2	7.05	7.70	3.50	2.90	4.10	3.23	5.59	6.86	3.40	9.07	1.92	10.0	5.50	4.39
Tb	n.d	n.d	0.70	1.61	1.69	0.98	1.07	n.d	0.39	n.d	0.42	0.65	0.90	0.43	1.23	0.24	1.49	n.d	0.58
Dy	3.70	4.40	3.39	7.80	7.73	4.83	5.20	2.40	1.56	2.70	1.87	3.12	4.33	1.98	5.91	1.18	6.92	3.70	2.69
Ho	0.64	0.73	0.63	1.36	1.42	0.86	0.85	0.46	0.28	0.45	0.35	0.55	0.74	0.35	1.04	0.19	1.21	0.66	0.51
Er	1.80	1.90	1.63	3.10	3.44	2.20	2.30	1.0	0.75	1.10	0.90	1.32	1.88	0.98	2.80	0.50	3.32	1.60	1.39
Tm	0.23	0.23	0.22	0.41	0.46	0.28	0.30	0.14	0.10	0.15	0.13	0.19	0.25	0.13	0.37	0.06	0.45	0.21	0.17
Yb	1.50	1.50	1.45	2.44	2.74	1.74	1.90	0.97	0.67	0.99	1.00	1.17	1.49	0.82	2.40	0.39	2.91	1.40	1.07
Lu	0.23	0.22	0.22	0.32	0.38	0.27	0.28	0.15	0.10	0.16	0.14	0.16	0.20	0.12	0.34	0.05	0.44	0.22	0.12

Abbreviations used are the same as in Table 1. The locations of the samples are shown in Fig. 2.

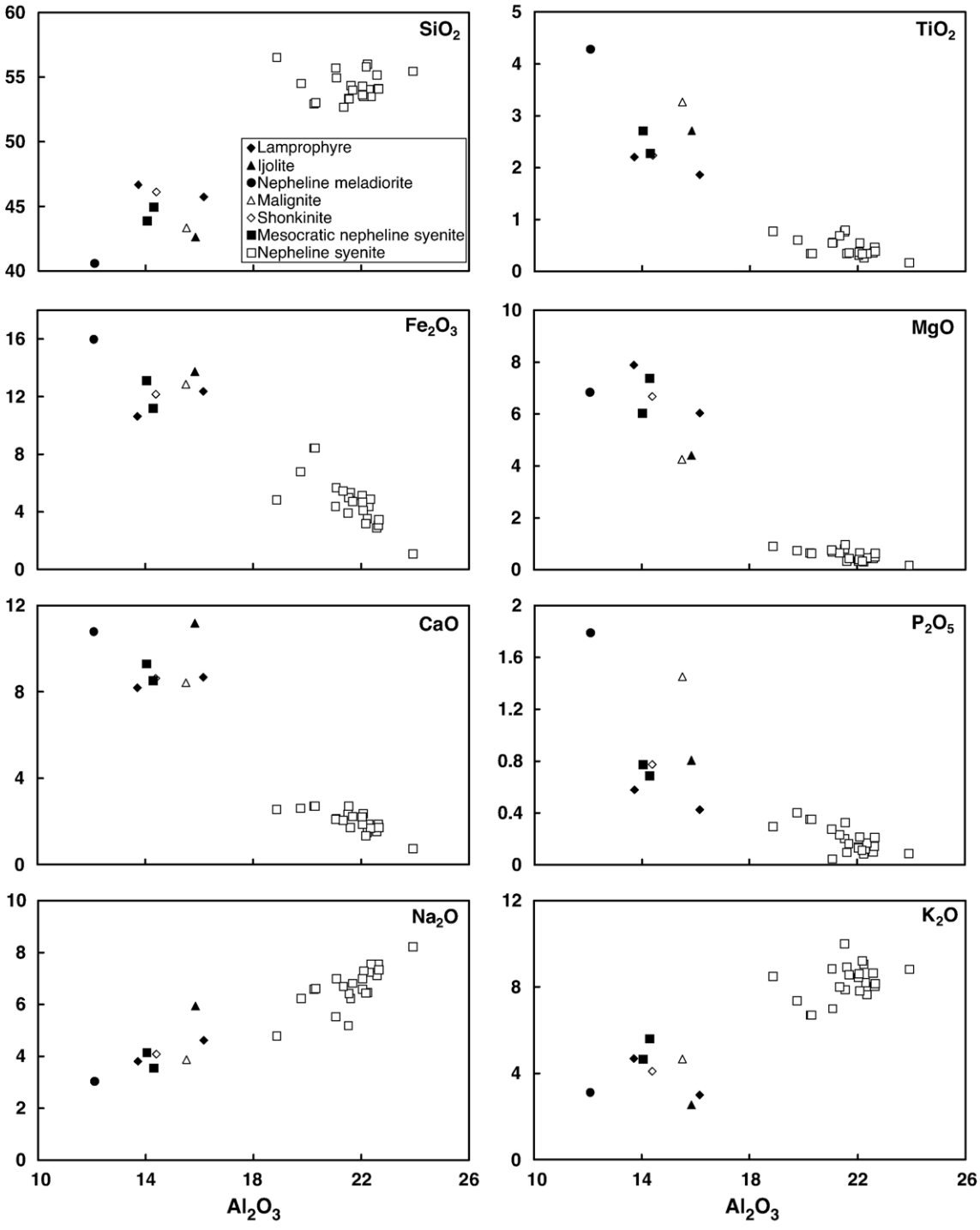

Fig. 6. Variation diagrams showing the trends in the major element chemistry of the Elchuru alkaline rocks.

SiO_2 increase with increase in Al_2O_3 content. MnO, MgO, Fe_2O_3, TiO_2, CaO and P_2O_5 decrease with increasing differentiation (Fig. 6). Similar trends are also seen in plots of the major oxides against the Differentiation Index, D.I. (defined as normative quartz + orthoclase + albite + nepheline + kalsilite + leucite; Thornton and Tuttle, 1969) (Fig. 7). A noteworthy feature is the general lack of rocks having

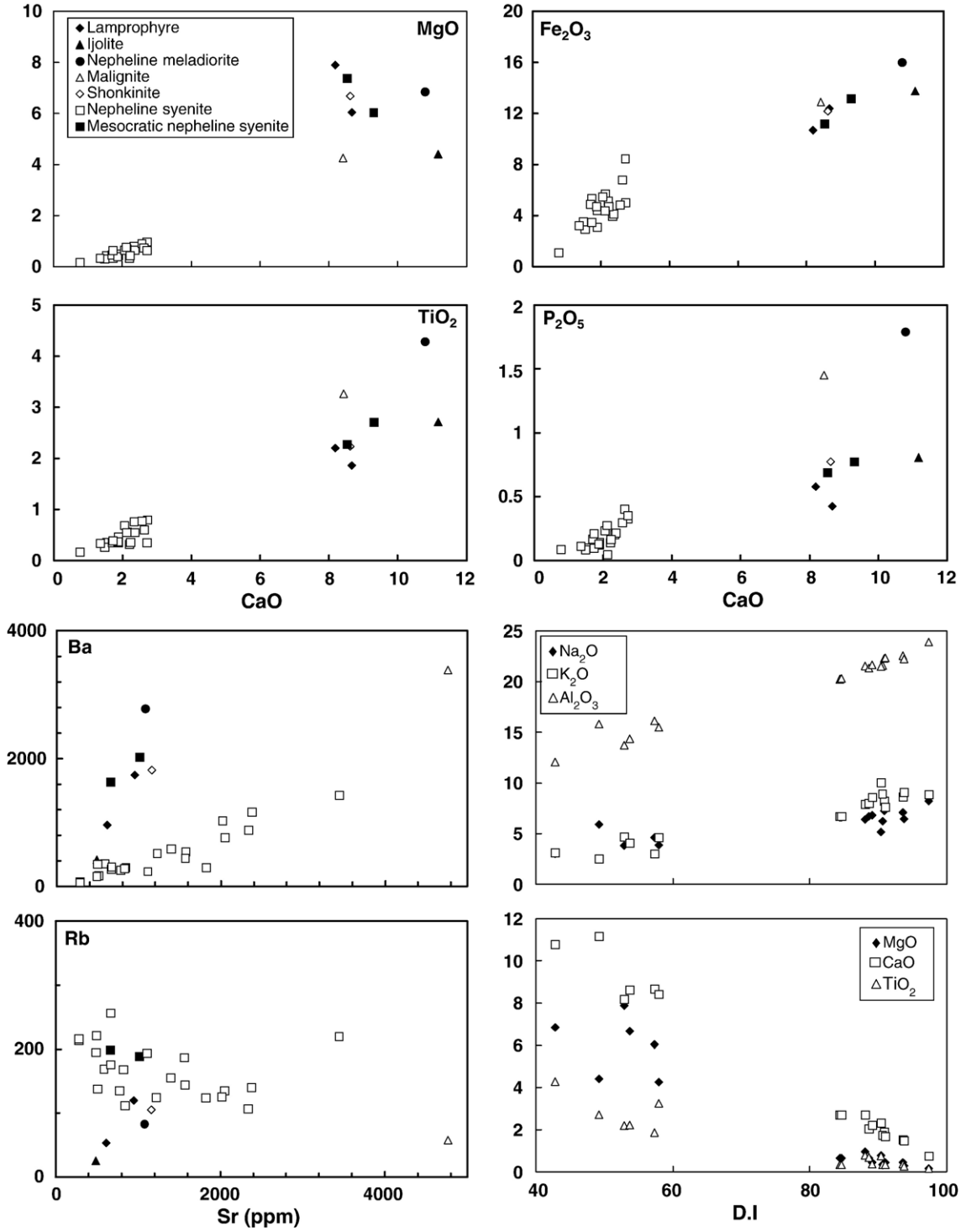

Fig. 7. Selected bivariate diagrams and plots of the major elements against D.I. (Thornton and Tuttle, 1969) for the Elchuru alkaline rocks.

compositions intermediate between the most evolved mafic member and the least evolved nepheline syenite.

The decrease in MgO and Fe_2O_3 concentrations with evolution suggests that crystal fractionation was dominated by mafic minerals (Fig. 6). This is also seen from the correlations of CaO with MgO and Fe_2O_3 which indicate the fractionation of Ca-bearing phases such as clinopyroxene and amphibole (Fig. 7). P_2O_5 and TiO_2

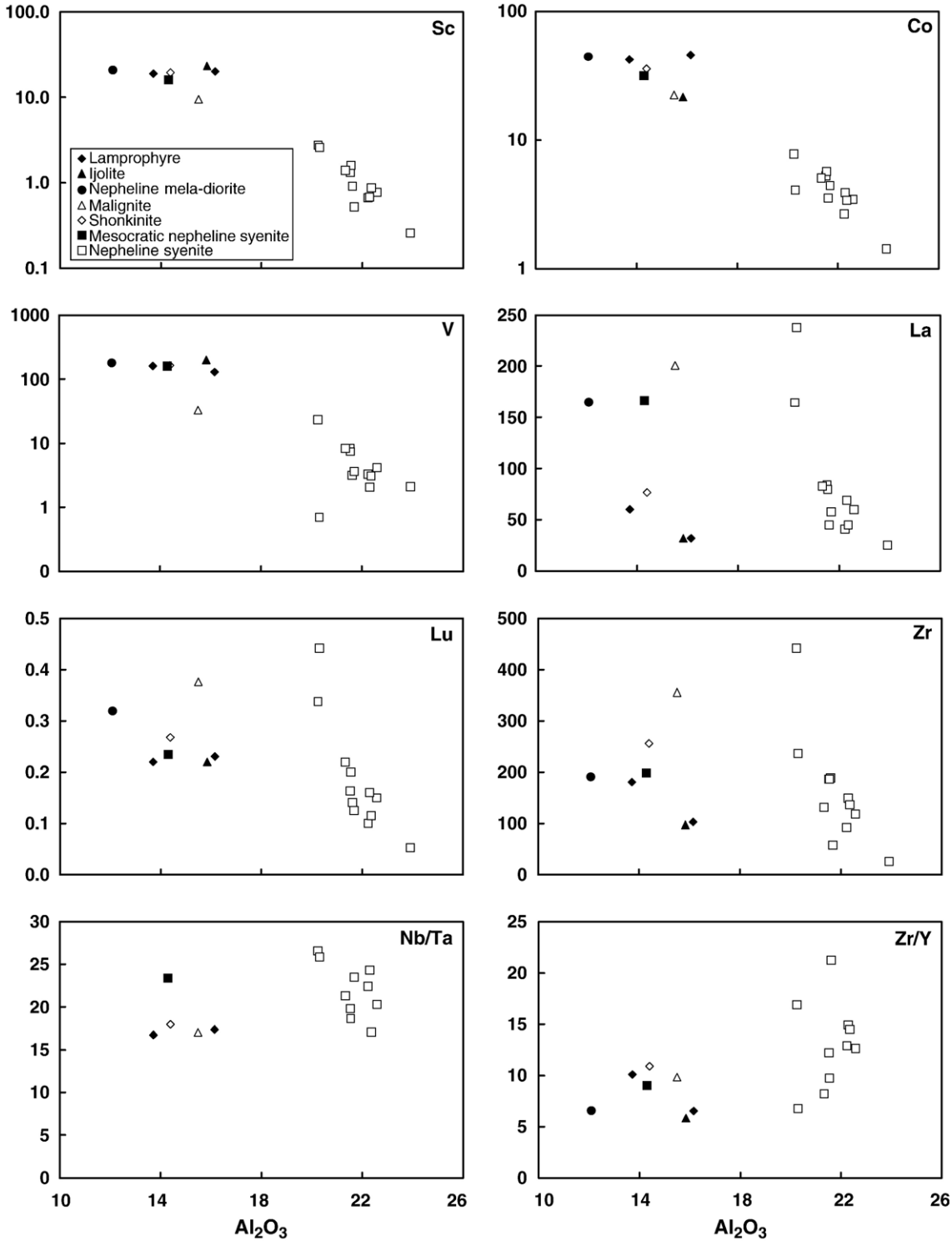

Fig. 8. Variation diagrams showing the trends in the trace element chemistry of the Elchuru alkaline rocks.

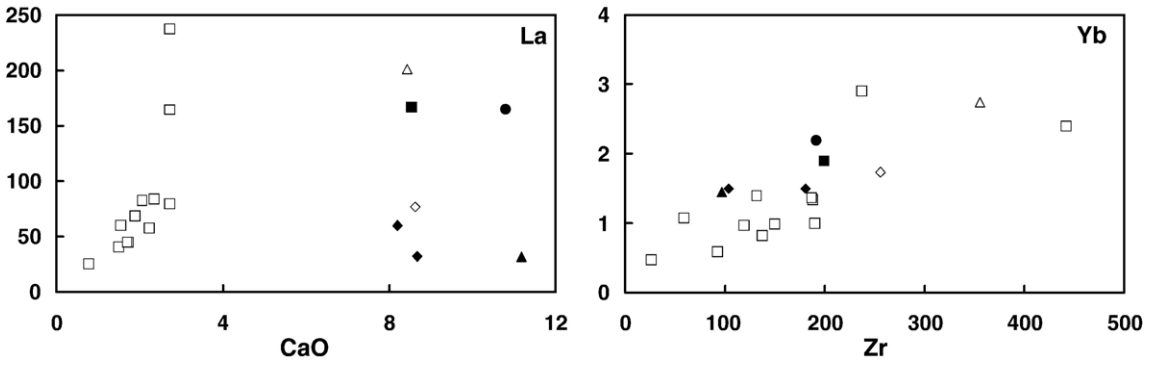

Fig. 8 (*continued*).

concentrations also decrease and show positive correlations with CaO, suggesting that apatite and titanite were important fractionating phases (Figs. 6 and 7). The increase of Na_2O and K_2O with differentiation indicates that alkali feldspar fractionation was not significant (Fig. 6). Similarly, the increase of Al_2O_3 and its negative correlation with CaO suggests that plagioclase fractionation was also minimal. The mafic members of the suite show a scatter in the trends for oxides like MgO, Fe_2O_3, TiO_2, CaO and P_2O_5 which may be due to the presence of cumulus crystals of clinopyroxene, amphibole, titanite and apatite. They have low Mg# (40–59) and lower Ni (2.2–143 ppm) and Cr (15.5–396 ppm) concentrations than primary mantle melts and show large variations in both the incompatible and the compatible element concentrations.

The nepheline syenites display coherent variations of the major and trace elements and define a differentiation series. They have extremely low Mg# (11–29) and show a 5–11 times decrease in the compatible element concentrations like Sc, Co and V which indicates that their evolution was dominated by fractional crystallization (Fig. 8). Many of the normally incompatible elements, especially the REE, also show a large variation in the group with concentrations decreasing with differentiation. La abundances decrease sharply and show a positive correlation with CaO, which may be indicative of allanite in the fractionating assemblage (Fig. 8). The Yb and Lu concentrations also show depletion and are positively correlated with Zr suggesting that the HREE budget was controlled by zircon fractionation (Fig. 8). No clear Zr trend is seen in the mafic rocks, implying that these rocks have not fractionated zircon. The Nb/Ta ratios in the nepheline syenites (17–27) are generally higher than those in the mafic rocks (16–20, Fig. 8). The decoupling of the 'geochemical twins' leading to an increase of the Nb/Ta ratio in the nepheline syenites indicates the removal of a phase that fractionates Ta from Nb. Experimental data (Green and Pearson, 1987; Prowatke and Klemme, 2005) suggest that such a phase could have been titanite which also explains the positive correlation of CaO with TiO_2 (Fig. 7). A similar positive correlation between P_2O_5 and CaO implies apatite fractionation, which, together with titanite can account for the decrease in the MREE abundances in the nepheline syenites. The Zr/Y ratios (7–21) of the nepheline syenites increase with evolution and are higher than those for the mafic rocks (6–11) (Fig. 10). The increase of Zr/Y requires the removal of a phase which can scavenge Y in preference to Zr (i.e., $K_D^{Zr/Y} < 1$) such as amphibole, garnet and clinopyroxene. Garnet being absent in the mineral assemblage can be ruled out as a fractionating phase. The increase of the Zr/Y ratios can hence be attributed to amphibole and clinopyroxene fractionation which, due to the strong affinity of these minerals for Fe (McBirney, 1993), also explains the depletion in Fe with differentiation. Sr, Ba and Rb show scatter on variation diagrams (Fig. 7); Sr and Ba are positively correlated with two perceptible trends in which Ba is more incompatible than Sr. The trend defined by the nepheline syenites has a lower Ba/Sr ratio in comparison to the mafic rocks indicating mineralogical control or different bulk K_D values (Fig. 7). In summary, the large variation of the trace elements seen in the nepheline syenite group can be accounted for by the fractionation of clinopyroxene and amphibole together with minor amounts of the accessory phases titanite, apatite, zircon and allanite. Two of the alkaline rock samples (899, malignite; 909, nepheline syenite) are extremely enriched in the REE. The REE spike in these samples is due to the high modal abundance of accessory phases some of which may be

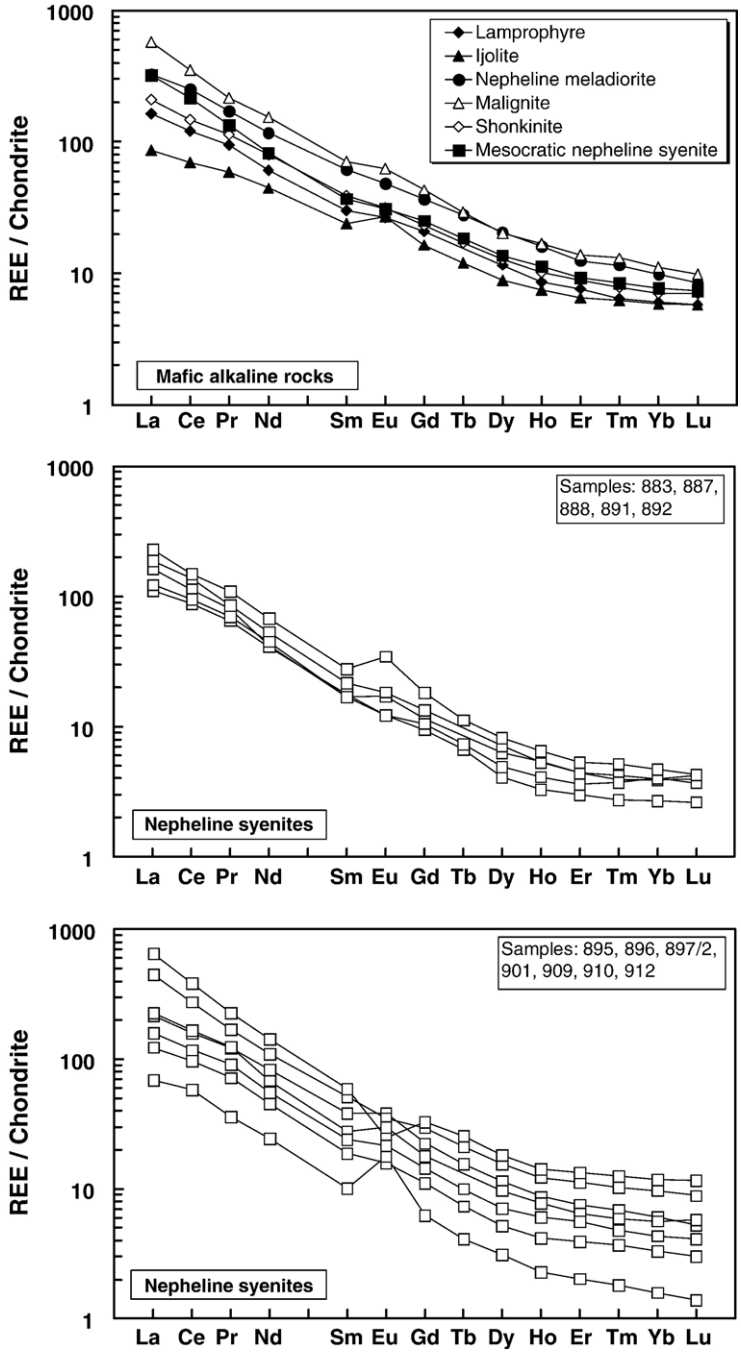

Fig. 9. Chondrite normalized REE patterns for more mafic alkaline rocks and nepheline syenites from the Elchuru alkaline complex. The normalizing values are taken from Taylor and McLennan (1985). Note the slightly convex upward patterns for the MREE in some mafic rocks and a complementary concave upward pattern for a few nepheline syenites.

cumulus crystals, as is seen in the malignite which has abundant apatite and titanite.

The enrichment of the light REE results in moderately steep REE patterns on chondrite normalized diagrams (Fig. 9). The absence of a prominent Eu anomaly in most rock types together with the Na, K and Al trends confirms that magmatic evolution was not dominated by plagioclase and alkali feldspar fractionation. The REE spectra of the malignite, shonkinite, mesocratic nepheline syenite and the lamprophyre show a slight upward

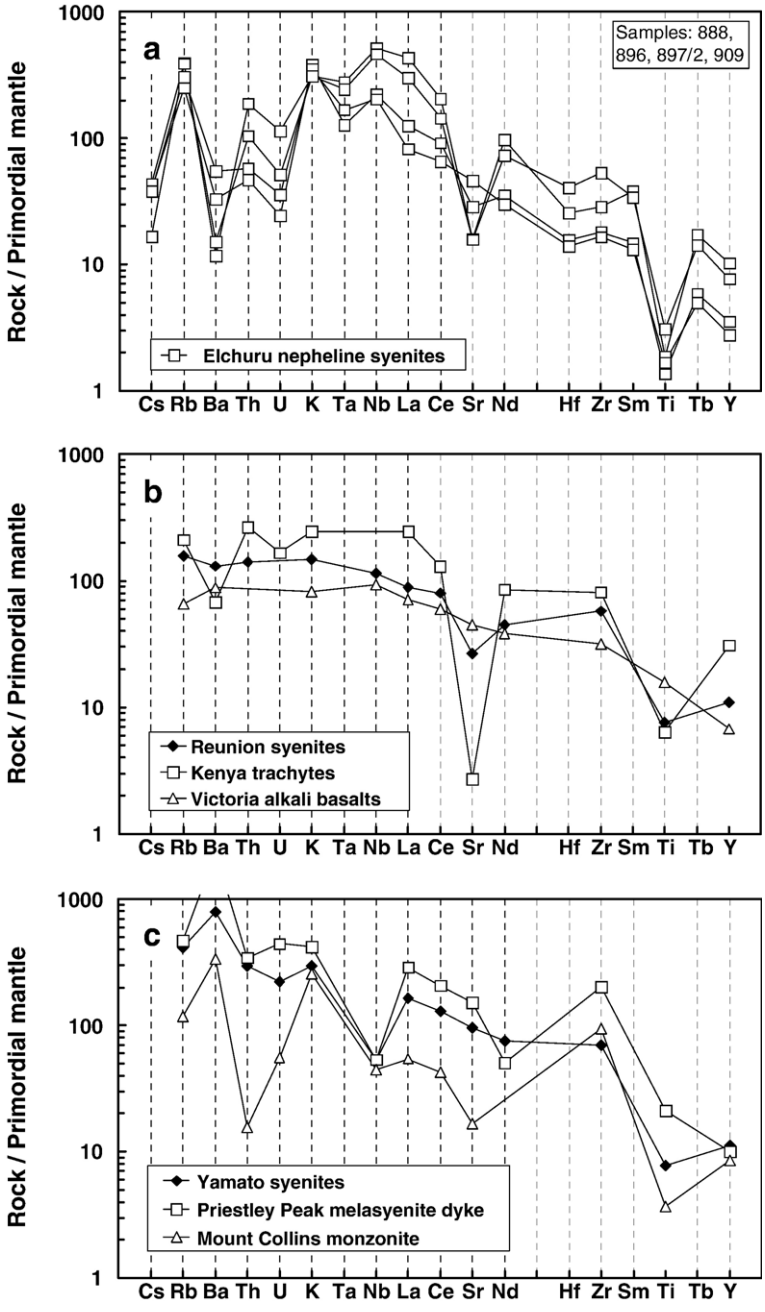

Fig. 10. Primitive-mantle normalized multi-element diagrams for (a) Elchuru nepheline syenites, (b) alkaline rocks from rift/hotspot-related tectonic settings (McDonough et al., 1985; Baker, 1987; Fisk et al., 1988) and (c) alkaline rocks from subduction zone settings (Sheraton and England, 1980; Zhao et al., 1995). The normalizing values are after Taylor and McLennan (1985).

convexity at the middle REE which can be attributed to the presence of minor cumulus crystals of apatite and titanite. Few nepheline syenite samples show a complementary slightly concave upward MREE pattern which is the effect of titanite, apatite and amphibole fractionation (Frey et al., 1978; Simmons and Hedge, 1978; Gleason et al., 1994). Even though the REE abundances in the nepheline syenites decrease with increasing differentiation, the patterns remain broadly parallel. This requires the fractionating assemblage to have bulk partition coefficient values which are quite similar and greater than one for all the REE.

Multi-element diagrams normalized to primitive mantle for some of the nepheline syenite samples are

Table 4
Rb–Sr, Sm–Nd and Pb isotope data of Elchuru alkaline rocks

Sample	Rock type	Rb (ppm)	Sr (ppm)	Sm (ppm)	Nd (ppm)	$^{87}Rb/^{86}Sr$	$^{87}Sr/^{86}Sr$	$2\sigma_{mean}$	$^{147}Sm/^{144}Nd$	$^{143}Nd/^{144}Nd$	$2\sigma_{mean}$	T_{DM} (Ma)	$(^{87}Sr/^{86}Sr)_i$	$(^{143}Nd/^{144}Nd)_i$	ε_{Ndi}
884	Lamp	53.1	613.3	4.45	24.91	0.250	0.708637	0.000013	0.10798	0.511734	0.000004	1987	0.703900	0.510797	−2.6
885	Lamp	120	947.0	6.98	43.29	0.367	0.710542	0.000010	0.09745	0.511575	0.000004	2014	0.703598	0.510729	−4.0
894	Ne-mel-dt	83.2	1077	14.1	83.36	0.223	0.707948	0.000019	0.10238	0.511587	0.000005	2085	0.703726	0.510698	−4.6
899	Malignite	58.1	4768	16.4	108.5	0.035	0.704697	0.000010	0.09128	0.511548	0.000005	1948	0.704031	0.510756	−3.4
905	Shonkinite	105	1160	8.95	56.39	0.262	0.708661	0.000012	0.09599	0.511553	0.000006	2017	0.703702	0.510720	−4.1
890	Mes.Ne-sye	189	1012	8.50	58.80	0.541	0.713712	0.000012	0.08737	0.511492	0.000005	1955	0.703475	0.510734	−3.9
883	Ne-syenite	135	775.2	3.91	29.75	0.504	0.712878	0.000012	0.07943	0.511436	0.000004	1904	0.703330	0.510747	−3.6
887	Ne-syenite	169	582.1	4.10	29.18	0.841	0.719083	0.000018	0.08485	0.511449	0.000004	1967	0.703157	0.510713	−4.3
888	Ne-syenite	127	506.3	5.01	37.49	0.727	0.717806	0.000013	0.08077	0.511465	0.000005	1891	0.704040	0.510764	−3.3
891	Ne-syenite	222	492.1	3.90	31.96	1.31	0.727212	0.000013	0.07383	0.511463	0.000004	1802	0.702445	0.510823	−2.1
892	Ne-syenite	220	3442	6.38	48.18	0.185	0.707349	0.000015	0.08005	0.511484	0.000005	1860	0.703847	0.510790	−2.8
895	Ne-syenite	140	2378	8.86	58.65	0.170	0.707165	0.000017	0.09133	0.511545	0.000005	1953	0.703940	0.510752	−3.5
896	Ne-syenite	168	821.0	4.34	32.21	0.593	0.714763	0.000013	0.08145	0.511485	0.000005	1878	0.703545	0.510778	−3.0
901	Ne-syenite	124	1821	2.33	17.29	0.197	0.707652	0.000016	0.08145	0.511541	0.000005	1815	0.703922	0.510835	−1.9
910	Ne-syenite	144	1570	6.41	48.65	0.265	0.708789	0.000019	0.07963	0.511513	0.000005	1823	0.703764	0.510822	−2.2
912	Ne-syenite	187	1562	5.54	39.44	0.347	0.710369	0.000012	0.08484	0.511466	0.000005	1948	0.703809	0.510730	−4.0
903	Fenitized c.r.	102	1769	8.77	60.61	0.167	0.712977	0.000011	0.08745	0.511453	0.000005	2001	0.709816	0.510695	−4.6

Sample	Rock type	$^{206}Pb/^{204}Pb$	$2\sigma_{mean}$	$^{207}Pb/^{204}Pb$	$2\sigma_{mean}$	$^{208}Pb/^{204}Pb$	$2\sigma_{mean}$
912	Ne-syenite	15.92	0.007	15.28	0.006	35.94	0.006
910	Ne-syenite	15.80	0.28	15.25	0.29	35.81	0.29
883	Ne-syenite	16.34	0.04	15.30	0.04	36.68	0.04
891	Ne-syenite	15.85	0.36	15.20	0.38	36.07	0.36

'i' refers to the initial isotopic ratios calculated at 1321 Ma. T_{DM} is the depleted mantle model age after Goldstein et al. (1984). The Pb isotopic data is from leached feldspar separates. Abbreviations same as in Table 1. c.r.=country rock.

shown in Fig. 10a. The patterns have distinct positive Nb anomalies, and negative Ti, Ba and Sr anomalies. The enrichment of Nb and Ta and the negative Ba and Sr anomalies rule out the involvement of subduction related processes in their evolution (Rogers et al., 1985; Nelson and McCulloch, 1989; Zhao et al., 1995). This is because alkaline rocks in such settings tend to have strong negative Nb and Ta anomalies as is seen for the Yamato syenites, Mount Collins monzonite (Zhao et al., 1995) and Priestley Peak melasyenite dykes (Sheraton and England, 1980) which are all interpreted to have subduction related tectonic affinities (Fig. 10c). In contrast, multi element patterns of rocks from rift or hot spot related tectonic setting like the Reunion syenites (Fisk et al., 1988), Kenya trachytes (Baker, 1987) and Victoria alkali basalts (McDonough et al., 1985) are enriched in Nb and Ta (McDonough et al., 1985; Menzies, 1987) which suggests a rift or hotspot related setting for the alkaline magmatism at Elchuru (Fig. 10b).

7. Sr, Nd and Pb isotopic signatures

Whole rock samples spanning the complete range of alkaline compositions including a fenitized country rock in the vicinity of the alkaline body were analyzed for their Sr and Nd isotopic ratios. Lead isotope ratios of leached feldspar separates were measured on four nepheline syenite samples. The data are presented in Table 4.

There exists no correlation between the isotopic ratios and rock types. The lack of any binary mixing relationship in plots between $(^{87}Sr/^{86}Sr)_i$ and 1/Sr and $(^{143}Nd/^{144}Nd)_i$ against 1/Nd (figures not shown) rules out any likelihood that the isotopic ratios define a two component mixture.

The calculated initial $^{87}Sr/^{86}Sr$ at 1321 Ma ranges from 0.702445 to 0.704040 while the initial $^{143}Nd/^{144}Nd$ varies between 0.510698 and 0.510835 corresponding to a narrow range of initial ε_{Sr} (−21.4 to 1.3; DePaolo, 1988) and ε_{Nd}^{CHUR} values (−4.6 to −1.9; Wasserburg et al., 1981). The initial isotopic ratios define a narrow field in the third quadrant of the Sr–Nd diagram and show signatures similar to or more enriched than EM-I ocean island basalts (Zindler and Hart, 1986; Hart, 1988) at 1321 Ma (Fig. 11). The fenitized garnet–hornblende gneiss from the country rock has high $^{87}Sr/^{86}Sr$ which is decoupled from Nd. One nepheline syenite (sample 891) has unusually low initial $^{87}Sr/^{86}Sr$ (0.702445) although its ε_{Nd} lies in the range for the alkaline suite, which may be attributed to disturbance in the Rb–Sr system during the Pan-African metamorphism. All the other rock types define a narrow cluster on the Sr–Nd diagram. The very homogenous Sr–Nd isotope data for the alkaline rocks indicate that they were derived from one homogenous source.

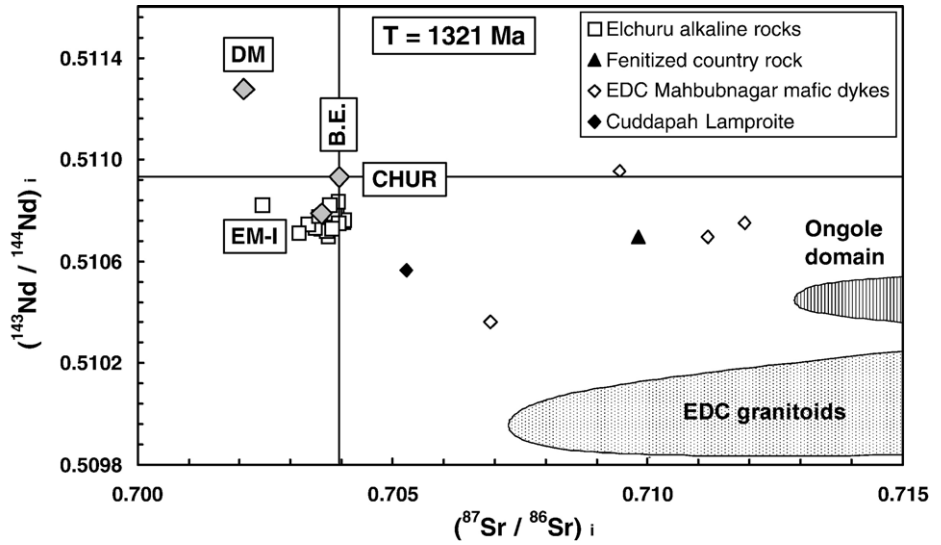

Fig. 11. Initial $^{143}Nd/^{144}Nd$ vs. $^{87}Sr/^{86}Sr$ diagram for the Elchuru alkaline rocks calculated at 1321 Ma. Also shown in the diagram are the approximate positions of the other important mantle reservoirs: depleted mantle, DM (Goldstein et al., 1984; Rehkämper and Hofmann, 1997) and Bulk Earth/Chondrite, CHUR (Wasserburg et al., 1981; DePaolo, 1988). Isotope ratios from rocks in the neighboring crustal domains are also plotted for reference. These include data from granitoids (Jayananda et al., 2000; Rickers et al., 2001), mafic dykes (Pandey et al., 1997) and a Cuddapah basin lamproite (Chalapathi Rao et al., 2004) from the Eastern Dharwar Craton (EDC) and felsic granulites from the Ongole domain of the Eastern Ghats Belt (EGB) (Rickers et al., 2001). The EDC and Ongole fields extend further beyond the upper limit of the Sr isotopic ratios shown in the diagram. The Elchuru alkaline rocks define a narrow field in the enriched quadrant and have isotopic ratios similar to OIB.

The Pb isotopic ratios measured on leached feldspars from the nepheline syenites are quite unradiogenic (Table 4). The measured $^{206}Pb/^{204}Pb$ (15.80–16.34), $^{207}Pb/^{204}Pb$ (15.20–15.30) and $^{208}Pb/^{204}Pb$ (35.81–36.68) ratios are illustrated graphically in $^{207}Pb/^{204}Pb$ vs. $^{206}Pb/^{204}Pb$ and $^{208}Pb/^{204}Pb$ vs. $^{206}Pb/^{204}Pb$ diagrams (Fig. 12). The low Pb ratios suggest that the feldspars have not completely re-equilibrated with the whole rock in spite of the medium grade metamorphic overprint on the rocks. In such circumstances, the measured Pb isotopic compositions of the feldspars would be reflective of the magma from which they crystallized and its source. The ratios are much lower than those of the exposed crust in the vicinity of the alkaline rocks and indicate that the local crust was not a contaminant and the two had different mantle sources. Assuming a single stage Pb growth model and using the isotopic ratios of Pb in troilite of Canyon Diablo for the primeval Pb composition (Tatsumoto et al., 1973), an average model age of 1225 Ma is obtained for three of the four feldspar samples from the nepheline syenites. Since the Pb model age is younger than the intrusion age of 1321 Ma for these rocks, a single stage Pb growth model requires that the source rock for the Elchuru alkaline magma had evolved with a μ value slightly higher than 8.

8. Petrogenetic discussion

8.1. Trace element and isotopic constraints on the source region

The enrichment of the LIL and HFS elements and the steep REE patterns of the rocks cannot be produced by any crystal fractionation mechanism from a parent

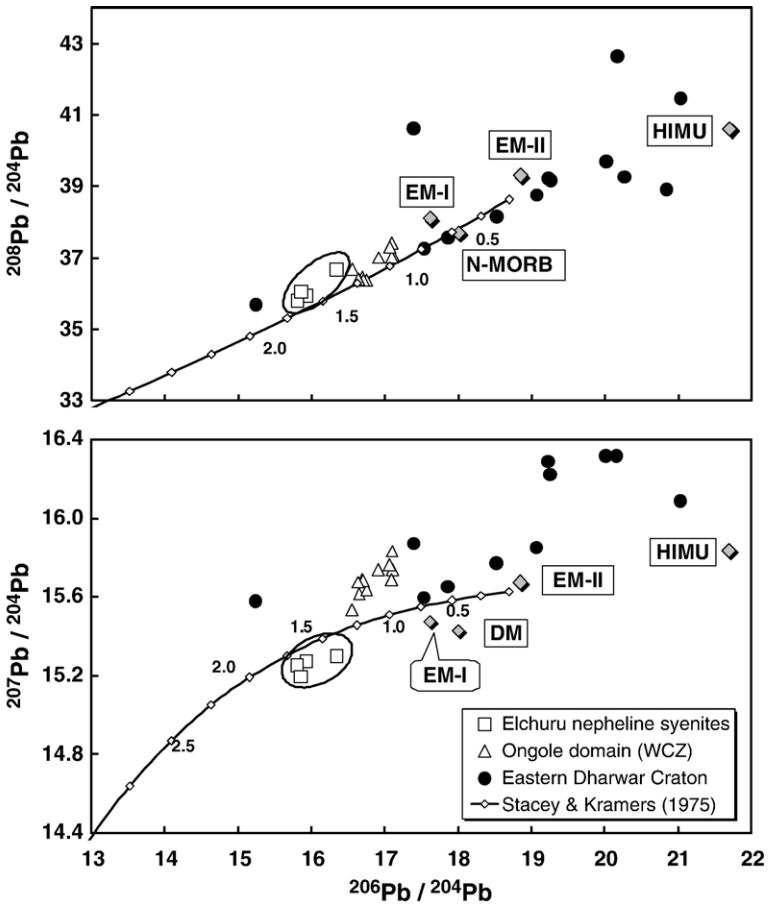

Fig. 12. Pb isotopic ratios of leached feldspar separates from nepheline syenites of the Elchuru alkaline complex. The diagram also shows the two stage terrestrial Pb evolution curves after Stacey and Kramers (1975) and the approximate present day positions of the different mantle reservoirs (Hart, 1988; Rehkämper and Hofmann, 1997). Whole rock and leached feldspar Pb isotope data from the Eastern Dharwar Craton (Pandey et al., 1997; Rickers et al., 2001) and the Ongole domain (Rickers et al., 2001) south of the Godavari rift are also shown for comparison. The feldspars from Elchuru are less radiogenic than those from the EDC (both leached feldspars and whole rock) and the Ongole domain which suggest that the mantle source region of the Elchuru alkaline rocks was different from the neighboring crustal domains.

magma depleted in these elements. The enrichment is also not due to crustal assimilation because the REE abundances are higher than in normal crustal material, thus, adding such material would actually diminish the REE content of the rocks. Moreover, the Sr, Nd and Pb isotopic ratios do not show any mixing relationship. Hence, it can be argued that the enrichment of the LIL, HFS and LRE elements is a characteristic of the source region. The Nb/Ta ratios of the rocks (16–27) lie typically in the range of sub-continental lithospheric mantle values (16–20; Weyer et al., 2002, 2003; Münker et al., 2003) while the Zr/Hf ratios (32–45) are mostly higher than chondritic values.

Although the Nd and Sr isotopic ratios do not provide an unambiguous constraint on a crustal or mantle source for these rocks, the low Pb isotope ratios from feldspars are indicative of a source that is relatively unradiogenic. Since nepheline syenites cannot be produced by the partial melting of normal crustal rocks, the obvious source for the alkaline rocks would be the upper mantle. Jayananda et al. (2000) have obtained single zircon evaporation Pb–Pb ages ranging between 2467 and 2540 Ma for the Hoskote Kolar granites in the EDC which can be approximated to represent the cratonic crust in the vicinity of the Elchuru alkaline complex at the time of its intrusion. Similarly, granulite facies felsic orthogneisses from the Ongole domain to the east of the Elchuru alkaline complex have DM model ages varying between 1800 and 2300 Ma (Rickers et al., 2001) and hence represent the Eastern Ghats crust in this segment at 1321 Ma. The time integrated evolution of the Elchuru alkaline rocks and the neighboring crustal domains (i.e., the EDC and the Ongole domain) can be illustrated in a $^{143}Nd/^{144}Nd$ vs. time diagram (Fig. 13). The initial Nd isotopic ratios of the alkaline rocks are distinctly higher than those of the exposed Late Archean to Early Proterozoic crust of the EDC and the EGB in its vicinity which clearly indicates that these crustal domains were not a component of the source region for Elchuru alkaline magma (Fig. 13). This is also evident from the low Pb isotope ratios of the Elchuru alkaline rocks which suggest that the source for the parent magma was less radiogenic than that for the neighboring crustal domains. Two component mixing calculations indicate that the Nd isotopic ratios of the alkaline rocks can only be explained by unrealistically high contamination (10–35%) of a depleted mantle (DM) derived melt with N-MORB like isotopic ratios by EDC crust, or by 20–54% contamination of a DM melt by Ongole domain crust. The resultant mixtures however would have a wide range of $^{87}Sr/^{86}Sr$ ratios all greater than 0.7049. This is in contrast to the well constrained $^{87}Sr/^{86}Sr$ ratios of the alkaline rocks which are less than 0.7040. Moreover, it is to be expected that such high amounts of crustal contamination would affect the mineralogy and introduce heterogeneity and mixing relationships in the Sr, Nd and Pb isotopic ratios, evidences for which are lacking. Integrating the geochemical data with the Sr–Nd and Pb isotopic constraints, the most reasonable source for the parental magma is a mantle enriched in LILE, HFSE and the LREE. Such a mantle could have been a part of the sub-continental lithosphere. The presence of a

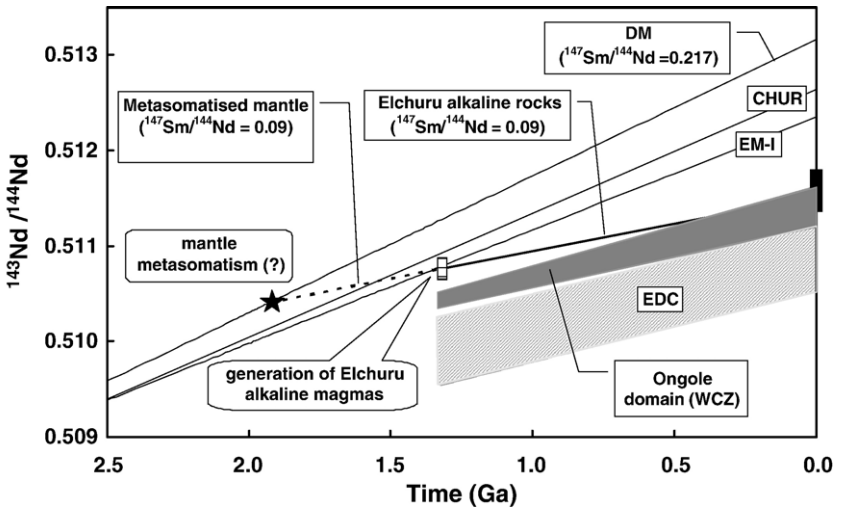

Fig. 13. Nd vs. time evolution diagram for the Elchuru alkaline rocks and the time integrated evolutionary curves for depleted mantle (DM), CHUR, enriched mantle (EM-I) and the neighboring crustal domains, i.e., granitoids from the EDC (Jayananda et al., 2000; Rickers et al., 2001) and felsic granulites from the Ongole domain (Rickers et al., 2001). See text for discussion.

Mesoproterozoic enriched mantle beneath the EDC is supported by Chalapathi Rao et al. (2004) who have obtained enriched Sr–Nd isotopic ratios (ε_{Nd}=−6.3 to −7.2; ε_{Sr}=3.3 to 51.5) for 1.4 Ga lamproite intrusives in the eastern parts of the Cuddapah basin. Nd isotopic data indicate that mantle enrichment in the EDC may have already started in the Paleoproterozoic as seen from the 2.5 Ga Closepet granite (Jayananda et al., 1995) and the 2.0 Ga enriched Hogenakal carbonatites (Kumar et al., 2004).

The unradiogenic Pb isotopic ratios for the Elchuru nepheline syenites suggest that the source rocks for the Elchuru parental magma had evolved with a low μ value. Coupled with the EM-I like Sr–Nd isotopic signatures and positive Nb–Ta anomalies, it is unlikely that the enrichment was caused by subducted oceanic crust and associated sediments. Hence, as suggested by Hart (1988) it is more likely that the EM-I like signature is the result of mantle metasomatism. The depleted mantle (DM) Nd model ages (after Goldstein et al., 1984) of the alkaline rocks range between 1801 and 2084 Ma (Table 4) and may represent the age of the enriched reservoir formed by metasomatism. Assuming that the metasomatising medium was isotopically indistinguishable from a depleted mantle at 1.9 Ga (corresponding to the model ages of the alkaline rocks), the source rock for the Elchuru alkaline magma (i.e., an enriched mantle) must have evolved with a $^{147}Sm/^{144}Nd$ ratio of about 0.09 to generate the desired isotopic ratios for the alkaline rocks at 1321 Ma (Fig. 13). Further fractionation of the Sm/Nd ratio during the extraction of the alkaline magma at 1321 Ma resulted in the observed $^{147}Sm/^{144}Nd$ ratios (0.0738–0.1079) for the Elchuru rocks.

9. Petrogenetic model

Large variations in the concentrations of the incompatible and compatible trace elements and the scatter in the major element trends for the mafic rocks indicate that their geochemical signatures may be a combined result of magmatic differentiation and accumulation of minor cumulus crystals. The evolution from mafic to felsic compositions in the alkaline suite can be modeled by a two-stage Rayleigh fractional crystallization scheme. The results of the fractional crystallization modeling are illustrated graphically in Fig. 14. The least evolved nepheline syenite (sample 897/2) is taken to represent the immediate parent magma for the nepheline syenites. The cumulus phase-free melanocratic nepheline diorite (sample 894) being one of the most enriched and least evolved members of the suite (Mg# 46) is taken to approximate the most primitive sampled parent magma. The first stage of the Rayleigh fractionation involving differentiation from such a parent magma to the least evolved nepheline syenite removes about 90% of the bulk rock MgO and hence ought to be dominated by the fractionation of Fe–Mg phases such as clinopyroxene and amphibole. Removing clinopyroxene (with 10.5 wt.% MgO) and amphibole (with 9.5 wt.% MgO) in the proportion 0.59 : 0.40 from such melts can produce magmas with #Mg similar to the least evolved nepheline syenite after about 90% crystallization. Although clinopyroxene and amphibole fractionation can explain the depletion of Fe–Mg, it cannot account for the variations of the trace elements, especially the REE. For example, removal of only clinopyroxene and amphibole cannot explain the simultaneous increase in La and Lu and decrease in Gd and Y concentrations. The elemental trends can, however, be satisfactorily explained by fractionating an assemblage consisting of about 59.6% clinopyroxene, 39.5% amphibole, 0.6% titanite, 0.2% apatite and 0.04% allanite. The second stage of fractional crystallization involving differentiation from the least evolved nepheline syenite to the most evolved one requires a drastic decrease of the 'incompatible' and compatible element concentrations and hence is likely to be controlled by accessory phases (which host the incompatible elements) in addition to clinopyroxene and amphibole. The observed elemental trends can be modeled by the fractionation of clinopyroxene (69.6%), amphibole (29%), titanite (0.8%), apatite (0.45%), allanite (0.1%) and zircon (0.1%). The involvement of zircon as a fractionating phase in this stage is also supported by the decreasing zirconium concentrations with differentiation. Interestingly, the second stage requires a higher bulk partition coefficient for Lu and lower bulk partition coefficients for Sc and Co in contrast to the reverse in the first stage which can be accommodated by changing the mineral–melt partition coefficients for Sc, Co and Lu in clinopyroxene. It is difficult to assess if this is an effect of changing partition coefficient with changing melt composition or a result of uncertainties in the partition coefficient data itself.

The formation of intermediate to syenitic magmas have been attributed to contrasting models that include either fractional crystallization of nephelinite or alkali basalt magmas (Bowen, 1928; Baker, 1987) or low degree partial melting of mantle and/or crustal rocks (Bailey and Schairer, 1966; Bailey, 1974; Price et al., 1985). Since the Elchuru alkaline rocks are geochemically evolved, possible models for their genesis include (i) fractional crystallization of an enriched alkali basalt

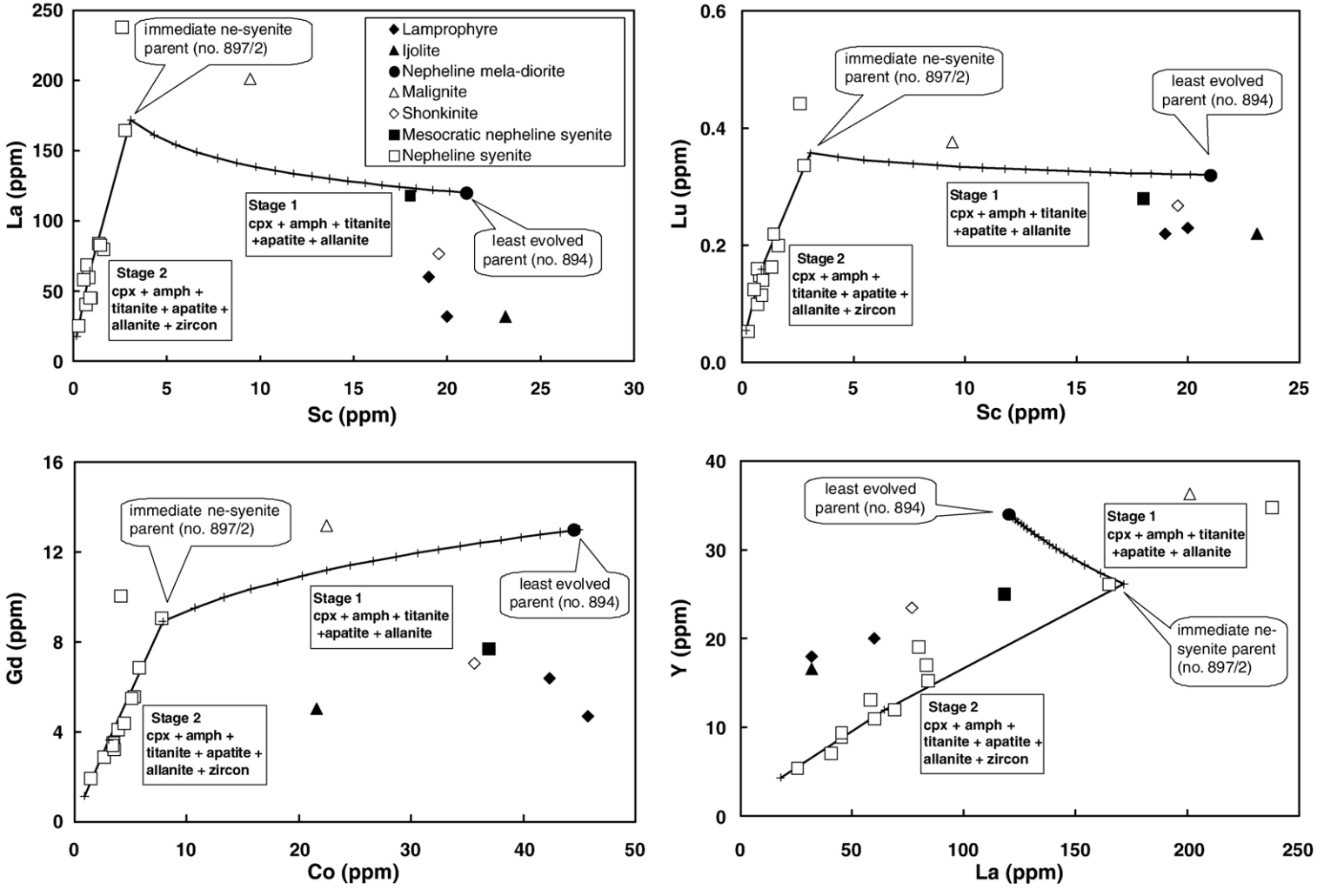

Fig. 14. Results of Rayleigh fractional crystallization modeling on the Elchuru alkaline suite. The geochemical variation from mafic to felsic compositions can be modeled by a two stage fractional crystallization scheme (See text for discussion). [Mineral–melt partition coefficients (D) were taken from: Paster et al. (1974) and Watson and Green (1981) for apatite, Lynton et al. (1993) and Prowatke and Klemme (2005) for titanite, Frey (1969), Nagasawa (1970), Ewart et al. (1973), Larsen (1979), Villemant et al. (1981), Green and Pearson (1983) and Hart and Dunn (1993) for clinopyroxene, Matsui et al. (1977), Lemarchand et al. (1987) and Green et al. (1993) for amphibole, Henderson (1982), Mahood and Hildreth (1983) and Ewart and Griffin (1994) for allanite and Mahood and Hildreth (1983), Fujimaki (1986) and Bea et al. (1994) for zircon.].

parent magma or (ii) fractional crystallization of an enriched nephelinite/basanitic parent magma.

Evolved alkaline magmas such as those representing the Elchuru nepheline syenites and associated mafic members (Mg# 11–59) can form by the fractional crystallization of an alkali basalt parent magma. The differentiation scheme requires large amounts of plagioclase fractionation producing characteristic negative Eu anomalies in the residual melts which increase with increasing REE abundances. Such a model has been proposed for the generation of the Ilimaussaq agpaite of the Gardar Alkaline Province in Greenland (Upton, 1987; Upton and Emeleus, 1987; Paslick et al., 1993), where mantle-derived primary magmas underwent fractionation to form the basaltic and hawaiitic magmas of the Gardar Province. Further differentiation of these melts at crustal pressures generated anorthosite cumulates and benmoreite magmas. Peralkaline melts are thought to have been formed by further fractionation aided by volatile transfer. The scheme, involving anorthoclase fractionation, explained the 'plagioclase effect' (Bowen, 1945) in these rocks which is documented by strong negative Eu anomalies. It is apparent however, that plagioclase or alkali feldspar fractionation had not played a dominant role in the evolution of the Elchuru alkaline rocks. This can be seen from the increase of Na, K and Al with differentiation and the lack of negative Eu anomalies in most of the rocks. Thus, it is unlikely that the parent magma for the Elchuru nepheline syenite had formed by the differentiation of an alkali basalt magma.

The lack of consistent and prominent negative Eu anomalies in most rocks requires a fractionation scheme in which plagioclase was not involved. Bailey (1987) has suggested that some salic magma may have an undisputable sub-continental mantle origin. The occurrence of lherzolite xenoliths in phonolites (Green et al., 1974; Irving and Price, 1981) and the presence of phonolitic and trachytic melt in mantle xenoliths (Edgar et al., 1989) also provide evidence in support of the mantle origin for many intermediate to felsic liquids. Green et al. (1974) have shown that 'mafic phonolite lava' (nepheline benmoreite) of Mt. Mitchell rocks in Australia having Mg# of about 55 and containing lherzolite inclusions with typical high pressure mineralogy might originate by crystal fractionation at high pressure within the upper mantle. The authors suggest that such intermediate magmas can be produced by the fractionation of kaersutitic amphibole as the dominant phase from basanitic parent magmas. Irving (1971) and Irving and Green (1972), from experimental studies on basanite and nepheline mugearite have shown that Ti-rich amphibole together with olivine, clinopyroxene and biotite occur as near liquidus phases for appropriate compositions and water content at pressures from 5–25 kb. Thus, these minerals can occur as potential fractionating phases in the evolution from basanitic to mugearitic and further evolved compositions. Such a model can elegantly account for the field and geochemical characteristics of the Elchuru alkaline rocks as well. Combined fractionation of kaersutitic amphibole and clinopyroxene at mantle pressures from a basanitic parent can produce melts lacking a negative Eu anomaly and with Mg# similar to the mafic rocks and the nepheline syenites at Elchuru. Fractionation of kaersutitic amphibole can also explain the strong negative Ti anomaly in the suite. The presence of Ti rich ferropargasite and ferrokaersutite in some of the nepheline syenites suggests that they were liquidus phases and further supports the above model. The apparent scarcity of mafic rocks in association with the nepheline syenites at Elchuru can be explained by the above model whereby the major part of magmatic evolution had taken place in the mantle before the nepheline syenite parent magma was finally emplaced in the crust. In the two-stage fractional crystallization, it is thus quite likely that the first stage involving evolution from the primitive parent magma to the least evolved nepheline syenite had taken place in the mantle while the second stage involving differentiation in the nepheline syenite group took place after the emplacement of the immediate nepheline syenite parent magma in the crust. This would also explain the lack of rocks defining the fractional crystallization trajectory in the first stage and the abundance of nepheline syenites defining the second stage of fractionation.

10. Conclusions

10.1. Petrogenetic summary

The alkaline intrusive complex of Elchuru was emplaced in an extensional tectonic setting at 1321 Ma and the alkaline rocks were deformed and metamorphosed to amphibolite-facies conditions during the Pan-African tectonothermal event. Major and trace elements coupled with Sr, Nd and Pb isotopic data indicate a multi-stage magmatic history for the alkaline rocks. The parent magma of the suite, similar in composition to the melanocratic nepheline diorite, was generated by in-mantle fractionation of kaersutitic amphibole and clinopyroxene from a basanitic primary magma. Its source region, a part of the sub-continental lithospheric mantle, was isotopically homogeneous and enriched in

the LILE, HFSE and the LREE. Further differentiation of the parent magma involved two stages of fractional crystallization. During the first stage, fractionation of clinopyroxene, amphibole, titanite, apatite and allanite formed some of the other mafic members of the suite as well as an evolved residual magma which was parental to the nepheline syenites. Further fractionation of clinopyroxene, amphibole, titanite, apatite, allanite and zircon from the residual magma led to the formation of the nepheline syenites. As a major part of magmatic evolution took place in the mantle, the general lack of mafic rocks in the field is to be expected.

10.2. Geodynamic implication

Alkaline magmatism at Elchuru may be the manifestation of a Mesoproterozoic continental breakup. The idea is supported by the rift-related geochemical signatures and Mesoproterozoic intrusion ages (TIMS and SHRIMP on zircons) of the alkaline complexes within the craton–EGB contact zone (Upadhyay et al., in press; Upadhyay and Raith, in press; present study; Upadyhyay and Raith, submitted for publication). The opening of a NE–SW trending Mesoproterozoic rift along the present cratonic margin could have formed an ocean towards the south and several craton margin basins (e.g., Chattisgarh basin, Indravati basin) where sediments were deposited in a riftogenic milieu on a stable Atlantic-type margin (Kale, 1991, 1995; Chaudhuri et al., 1999). It is also interesting to note that glauconite from sandstones of the lower sedimentary sequence in the Godavari–Pranhita graben yields a K–Ar age of 1330±53 Ma (Vinogradov et al., 1964). This age could be a minimum for the opening of the Godavari rift. If the Mesoproterozoic rifting along the cratonic margin and the formation of the Godavari–Pranhita graben are related, their broadly contemporaneous ages suggests that the Godavari graben may represent the failed arm of a rift system in which the NE–SW trending arm was the active segment. Such a geodynamic scenario has been supported by Dobmeier and Raith (2003) and can elegantly account for the requirement of a basin in which the sedimentary sequences of the Eastern Ghats Province were deposited before being deformed-metamorphosed to granulite-facies conditions during the Grenvillian orogeny. Chaudhuri and Deb (2004) on the basis of stratigraphic correlations and sedimentary signatures suggest that the Godavari rift valley deepened towards the southeast which served as the pathway for marine transgression and open marine circulation. Such a palaeogeographic situation in the Mesoproterozoic can only be explained if rifting along the cratonic margin opened an ocean towards the south.

Zhao et al. (2004) have postulated the existence of a Paleo-Mesoproterozoic supercontinent referred to as Columbia preceding the formation of Rodinia. The authors argue that this pre-Rodinian supercontinent was assembled along global 2.1–1.8 Ga collisional orogens and contained almost all of Earth's continental blocks. The extrusion of felsic lavas at 1.87–1.77 Ga in the Krishna Province is broadly coeval with the extended 1.8–1.3 Ga magmatic accretionary belts along the southern margin of North America, Greenland and Baltica which are interpreted to represent subduction-related growth of Columbia via accretion at continental margins (Zhao et al., 2004). The rift-related geochemical signatures and the Mesoproterozoic ages for the Elchuru and other alkaline bodies along the craton–EGB contact are also remarkably consistent with the postulated final breakup of Columbia at about 1.3–1.2 Ga. If the southern Indian cratons and their contiguous terranes had formed an integral part of the Proterozoic evolution of Columbia, the Mesoproterozoic alkaline magmatism along the cratonic margin may have been the manifestation of a Mesoproterozoic rift related to the disintegration of Columbia.

The terrane boundary between the Bhandara–EDC cratons and the EGB is marked by a series of thrusts with west vergent movement interpreted to result from the thrusting of the EGB granulites over the Indian shield. The zircon and biotite ages from the Elchuru alkaline rocks indicate that they were deformed and metamorphosed during Pan-African tectonism which was possibly related to the west-ward thrusting of the granulites. The superposition of a collisional regime on an earlier extension related one during Pan-African tectonism was an effect of the Pan-African orogeny which is clearly documented in many parts of Gondwanaland (Condie, 2003).

Acknowledgement

We would like to sincerely thank Dr. W. Czygan (University of Freiburg) for providing the samples and valuable information on field relations and Prof. J. Erzinger from GFZ, Potsdam for offering analytical facilities to perform ICP-MS and ICP-AES analyses on selected samples. D.U. is grateful to Ms. M. Feth and Ms. H. M. Baier for their help during the course of analytical work at Berlin and Münster. Special thanks are also due to our colleagues at the Mineralogisch–Petrologisches

Institut, Bonn, for their support during the course of the study. Field work of D.U. was supported through DAAD-DST PPP-project no. D/02/31713 and is duly acknowledged. Constructive comments from two anonymous reviewers are also acknowledged.

References

Aftalion, M., Bowes, D.R., Dash, B., Fallick, A.E., 2000. Late Pan-African thermal history in the Eastern Ghats Terrane, India, from U–Pb and K–Ar isotopic study of the Mid-Proterozoic Khariar alkali syenite, Orissa. Geological Survey of India Special Publication 57, 26–33.

Bailey, D.K., 1974. Continental rifting and alkaline magmatism. In: Sørenson, H. (Ed.), The Alkaline Rocks. Wiley, New York, pp. 148–159.

Bailey, D.K., 1987. Mantle metasomatism—perspective and prospect. In: Fitton, J.G., Upton, B.G.J. (Eds.), Alkaline Igneous Rocks. Geological Society Special Publication, vol. 30, pp. 1–13.

Bailey, D.K., Schairer, J.F., 1966. The system Na_2O–Al_2O_3–Fe_2O_3–SiO_2 at 1 atmosphere, and the petrogenesis of alkaline rocks. Journal of Petrology 7, 114–170.

Baker, B.H., 1987. Outline of the petrology of the Kenya Rift alkaline province. In: Fitton, J.G., Upton, B.G.J. (Eds.), Alkaline Igneous Rocks. Geological Society Special Publication, vol. 30, pp. 293–311.

Bea, F., Pereira, M.D., Stroh, A., 1994. Mineral/leucosome trace-element partitioning in a peraluminous migmatite (a laser ablation-ICP-MS study). Chemical Geology 117, 291–312.

Bhadra, S., Gupta, S., Banerjee, M., 2004. Structural evolution across the Eastern Ghats Mobile Belt–Bastar craton boundary, India. Hot over cold thrusting in an ancient collision zone. Journal of Structural Geology 26, 233–245.

Black, L.P., Kamo, S.L., 2003. TEMORA 1: a new zircon standard for U–Pb geochronology. Chemical Geology 200, 155–170.

Bowen, N.L., 1928. The Evolution of the Igneous Rocks. Princeton University Press.

Bowen, N.L., 1945. Phase equilibria bearing on the origin and differentiation of alkaline rocks. American Journal of Science 243, 75–89.

Chalapathi Rao, N.V., Miller, J.A., Pyle, D.M., Madhavan, V., 1996. New Proterozoic K–Ar ages for some kimberlites and lamproites from the Cuddapah Basin and the Dharwar Craton, South India: evidence for non-contemporaneous emplacement. Precambrian Research 79, 363–369.

Chalapathi Rao, N.V., Gibson, S.A., Pyle, D.M., Dickin, A.P., 2004. Petrogenesis of Proterozoic lamproites and kimberlites from the Cuddapah Basin and Dharwar Craton, Southern India. Journal of Petrology 45, 907–948.

Chaudhuri, A.K., Deb, G.K., 2004. Proterozoic rifting in the Pranhita–Godavari Valley: implication on India–Antarctica linkage. Gondwana Research 7, 301–312.

Chaudhuri, A.K., Mukhopadhyay, J., Deb, S.P., Chanda, S.K., 1999. The Neoproterozoic cratonic successions of Peninsular India. Gondwana Research 2, 213–225.

Chetty, T.R.K., Murthy, D.S.N., 1994. Collisional tectonics in the Late Precambrian Eastern Ghats Mobile Belt: mesoscopic to satellite-scale structural observations. Terra Nova 6, 72–81.

Condie, K.C., 2003. Supercontinents, super plumes and continental growth: the Neoproterozoic record. In: Yoshida, M., Windley, B.F., Dasgupta, S. (Eds.), Proterozoic East Gondwana: Supercontinent Assembly and Breakup. Geological Society Special Publication, vol. 206, pp. 1–21.

Czygan, W., Goldenberg, G., 1989. Petrography and geochemistry of the alkaline complexes of Sivamalai, Elchuru and Uppalapadu, India. Memoirs Geological Society of India 15, 225–240.

Dasgupta, S., Sengupta, P., 2003. Indo-Antarctic correlation: a perspective from the Eastern Ghats Belt. In: Yoshida, M., Windley, B.F., Dasgupta, S. (Eds.), Proterozoic East Gondwana: Supercontinent Assembly and Breakup. Geological Society Special Publication, vol. 206, pp. 131–143.

Dawson, J.B., 1987. The kimberlite clan: relationship with olivine and leucite lamproites, and inferences for upper mantle metasomatism. In: Fitton, J.G., Upton, B.G.J. (Eds.), Alkaline Igneous Rocks. Geological Society Special Publication, vol. 30, pp. 95–101.

DePaolo, D.J., 1988. Neodymium Isotope Geochemistry: An Introduction. Springer Verlag, New York.

Dobmeier, J.C., Raith, M.M., 2003. Crustal architecture and evolution of the Eastern Ghats Belt and adjacent regions of India. In: Yoshida, M., Windley, B.F., Dasgupta, S. (Eds.), Proterozoic East Gondwana: Supercontinent Assembly and Breakup. Geological Society Special Publication, vol. 206, pp. 145–168.

Edgar, A.D., 1987. The genesis of alkaline magmas with emphasis on their source regions: inferences from experimental studies. In: Fitton, J.G., Upton, B.G.J. (Eds.), Alkaline Igneous Rocks. Geological Society Special Publication, vol. 30, pp. 29–52.

Edgar, A.D., Lloyd, F.E., Forsyth, D.M., Barnett, R.L., 1989. Origin of glass in upper mantle xenoliths from the Quaternary volcanics of Gees, West Eifel, Germany. Contributions to Mineralogy and Petrology 103, 277–286.

Ewart, A., Griffin, W.L., 1994. Application of proton-microprobe data to trace-element partitioning in volcanic-rocks. Chemical Geology 117, 251–284.

Ewart, A., Bryan, W.B., Gill, J.B., 1973. Mineralogy and geochemistry of the younger volcanic islands of Tonga, S. W. Pacific. Journal of Petrology 14, 429–465.

Fisk, M.R., Upton, B.G.J., Ford, C.E., 1988. Geochemical and experimental study of the genesis of magma of Reunion Island, Indian Ocean. Journal of Geophysical Research 93, 4933–4950.

Fitton, J.G., 1987. The Cameroon Line, West Africa: a comparison between oceanic and continental alkaline volcanism. In: Fitton, J. G., Upton, B.G.J. (Eds.), Alkaline Igneous Rocks. Geological Society Special Publication, vol. 30, pp. 273–291.

Frey, F.A., 1969. Rare earth abundances in a high-temperature peridotite intrusion. Geochimica et Cosmochimica Acta 33, 1429–1447.

Frey, F.A., Chappel, B.W., Roy, S.D., 1978. Fractionation of rare earth elements in the Tuolumne Intrusive Series, Sierra Nevada batholith, California. Geology 6, 239–242.

Fujimaki, H., 1986. Partition-coefficients of Hf, Zr, and REE between zircon, apatite, and liquid. Contributions to Mineralogy and Petrology 94, 42–45.

Gleason, J.D., Miller, C.F., Wooden, J.L., Bennett, V.C., 1994. Petrogenesis of the highly potassic 1.42 Ga Barrel Spring pluton, southeastern California, with implications for Mid-Proterozoic magma genesis in the southwestern USA. Contributions to Mineralogy and Petrology 118, 182–197.

Goldstein, S.L., O'Nions, R.K., Hamilton, P.J., 1984. A Sm–Nd study of atmospheric dusts and particulates from major river systems. Earth and Planetary Science Letters 70, 221–236.

Green, T.H., Pearson, N.J., 1983. Effect of pressure on rare earth element partition coefficients in common magmas. Nature 305, 414–416.

Green, T.H., Pearson, N.J., 1987. An experimental study of Nb and Ta partitioning between Ti-rich minerals and silicate liquids at high pressure and temperatures. Geochimica et Cosmochimica Acta 51, 55–62.

Green, D.H., Edgar, A.D., Beasley, P., Kiss, E., Ware, N.G., 1974. Upper mantle source for some hawaiites, mugearites and benmoreites. Contributions to Mineralogy and Petrology 48, 33–43.

Green, T.H., Adam, J., Site, S.H., 1993. Proton microprobe determined trace element partition coefficients between pargasite, augite and silicate or carbonatitic melts. EOS 74, 340.

Grew, E.S., Manton, W.I., 1986. A new correlation of sapphirine granulites in the Indo-Antarctic metamorphic terrane: Late Proterozoic dates from the Eastern Ghats. Precambrian Research 33, 123–139.

Gupta, S., Bhattacharya, A., Raith, M., Nanda, J.K., 2000. Contrasting pressure–temperature-deformation history across a vestigial craton–mobile belt boundary: the western margin of Eastern Ghats Belt at Deobhog, India. Journal of Metamorphic Geology 18, 683–697.

Hamilton, D.L., Mackenzie, W.S., 1960. Nepheline solid solution in the system $NaAlSiO_4$–$KAlSiO_4$–SiO_2. Journal of Petrology 1, 56–72.

Hart, S.R., 1988. Heterogeneous mantle domains: signatures, genesis and mixing chronologies. Earth and Planetary Science Letters 90, 273–296.

Hart, S.R., Dunn, T., 1993. Experimental cpx/melt partitioning of 24 trace elements. Contributions to Mineralogy and Petrology 113, 1–8.

Henderson, P., 1982. Inorganic Geochemistry. Pergamon, Oxford, p. 353.

Irving, A.J., 1971. Geochemical and high pressure experimental studies of xenoliths, megacrysts and basalts from south eastern Australia. Unpublished Ph.D. thesis, Australian National University, Canberra.

Irving, A.J., Green, D.H., 1972. Experimental study of phase relationships in a high-pressure mugearitic basalt as a function of water content. Abstracts with Programs. Geological Society of America, 4, pp. 550–551.

Irving, A.J., Price, R.C., 1981. Geochemistry and evolution of high pressure phonolitic rocks from Nigeria, Australia, Eastern Germany and New Zealand. Geochimica et Cosmochimica Acta 45, 1309–1320.

Jayananda, M., Martin, H., Peucat, J.J., Mahabaleswar, B., 1995. Late Archaean crust–mantle interactions: geochemistry of LREE-enriched mantle derived magmas. Example of the Closepet batholith, southern India. Contributions to Mineralogy and Petrology 119, 314–329.

Jayananda, M., Moyen, J.F., Martin, H., Peucat, J.J., Auvray, B., Mahabaleswar, B., 2000. Late Archean (2550–2520 Ma) juvenile magmatism in the Eastern Dharwar craton, Southern India: constraints from geochronology, Nd–Sr isotopes and whole rock geochemistry. Precambrian Research 99, 225–254.

Kale, V.S., 1991. Constrains on the evolution of the Purana basins of Peninsular India. Journal of the Geological Society India 38, 231–252.

Kale, V.S., 1995. Association of the Purana basin and the middle Proterozoic mobile belts in Peninsular India: Implication of targeting uranium deposits. Exploration and Research for Atomic Minerals 8, 95–110.

Kovach, V.P., Simmat, R., Rickers, K., Berezhnaya, N.G., Salnikova, E.B., Dobmeier, C., Raith, M.M., Yakovleva, S.Z., Kotov, A.B., 2001. The Western Charnockite Zone of the Eastern Ghats Belt, India; an independent crustal province of Late Archean (2.8 Ga) and Paleoproterozoic (1.7–1.6 Ga) terrains. Gondwana Research 4, 666–667.

Kumar, A., Gopalan, K., Macdougall, J.D., 2004. Depleted and enriched mantle sources for Paleoproterozoic and Neoproterozoic carbonatites of southern India; Sr, Nd, C–O isotopic and geochemical constraints; discussion. Chemical Geology 213, 431–433.

Larsen, L.M., 1979. Distribution of REE and other trace-elements between phenocrysts and peralkaline undersaturated magmas, exemplified by rocks from the Gardar Igneous Province, South Greenland. Lithos 12, 303–315.

Leake, B.E., Woolley, A.R., Arps, C.E.S., Birch, W.D., Gilbert, C.M., Grice, J.D., Hawthorne, F.C., Kato, A., Kisch, H.J., Krivovichev, V.G., Linthout, K., Laird, J., Mandarino, J.A., Maresch, W.V., Nickel, E.H., Rock, N.M.S., Schumacher, J.C., Smith, D.C., Stephenson, N.C.N., Ungaretti, L., Whittaker, E.J.W., Youzhi, G., 1997. Nomenclature of amphiboles: report of the Subcommittee on Amphiboles of the International Mineralogical Association, Commission on New Minerals and Mineral Names. American Mineralogist 82, 1019–1037.

Leelanandam, C., 1980. An alkaline province in Andhra Pradesh. Current Science 49, 550–551.

Leelanandam, C., 1981. Some observations on the alkaline province of Andhra Pradesh. Current Science 50, 799–802.

Leelanandam, C., 1989. The Prakasam Alkaline Province in Andhra Pradesh, India. Journal of the Geological Society of India 34, 25–45.

Lemarchand, F., Benoit, V., Calais, G., 1987. Trace element distribution coefficients in alkaline series. Geochimica et Cosmochimica Acta 51, 1071–1081.

Ludwig, K.R., 1999. User's manual for Isoplot/Ex, Version 2.10, a geochronological toolkit for Microsoft Excel. Berkeley Geochronology Center Special Publication 1a, 2455 Ridge Road, Berkeley CA 94709, USA.

Ludwig, K.R., 2000. SQUID 1.00, a user's manual. Berkeley Geochronology Center Special Publication 2, 2455 Ridge Road, Berkeley, CA 94709, USA.

Lugmair, G.W., Shimamura, T., Lewis, R.S., Anders, E., 1983. Samarium-146 in the early solar system; evidence from neodymium in the Allende Meteorite. Science 222, 1015–1018.

Luhr, J.F., Carmichael, I.S.E., Varekamp, J.C., 1984. The 1982 eruptions of El Chichon Volcano, Chiapas, Mexico: mineralogy and petrology of the anhydrite-bearing pumices. Journal of Volcanology and Geothermal Research 23, 69–108.

Lynton, S.J., Candela, P.A., Piccoli, P.M., 1993. An experimental study of the partitioning of copper between pyrhotite and a high silica rhyolitic melt. Economic Geology and the Bulletin of the Society of Economic Geologists 88, 901–915.

Madhavan, V., Leelanandam, C., 1979. Hypersolvus and subsolvus rocks of the Elchuru alkaline pluton, Prakasam district, Andhra Pradesh, India. Neues Jahrbuch für Mineralogie Abhandlungen 136, 276–286.

Madhavan, V., Leelanandam, C., 1988. Petrology of the Elchuru Alkaline Pluton, Prakasam District, Andhra Pradesh, India. Journal of the Geological Society of India 31, 515–537.

Madhavan, V., Rao, J.M., Balaram, V., Kumar, R., 1992. Geochemistry and petrogenesis of lamprophyres and associated dykes from Elchuru, Andhra Pradesh, India. Journal of the Geological Society of India 40, 135–149.

Mahood, G.A., Hildreth, E.W., 1983. Large partition coefficients for trace elements in high-silica rhyolites. Geochimica et Cosmochimica Acta 47, 11–30.

Matsui, Y., Onuma, N., Nagasawa, H., Higuchi, H., Banno, S., 1977. Crystal structure control in trace element partition between crystal and magma. Tectonics 100, 315–324.

McBirney, A.R., 1993. Igneous Petrology. Jones and Bartlett Publishers, London, UK.

McDonough, W.F., McCulloch, M.T., Sun, S.S., 1985. Isotopic and geochemical systematic in Tertiary–Recent basalts from southeastern Australia and implications for the evolution of the subcontinental lithosphere. Geochimica et Cosmochimica Acta 49, 2051–2067.

Menzies, M., 1987. Alkaline rocks and their inclusions: a window on the Earths interior. In: Fitton, J.G., Upton, B.G.J. (Eds.), Alkaline Igneous Rocks. Geological Society Special Publication, vol. 30, pp. 15–27.

Mezger, K., Cosca, M., 1999. The thermal history of the Eastern Ghats Belt (India), as revealed by U–Pb and $^{40}Ar/^{39}Ar$ dating of metamorphic and magmatic minerals: implications for the SWEAT correlation. Precambrian Research 94, 251–271.

Mitchell, R.H., 1990. A review of the compositional variation of amphiboles in alkaline plutonic complexes. Lithos 26, 135–156.

Münker, C., Pfänder, J.A., Weyer, S., Büchl, A., Kleine, T., Mezger, K., 2003. Evolution of planetary cores and the Earth–Moon system from Nb/Ta systematics. Science 301, 84–87.

Nag, S., 1983. The alkaline rocks of Eastern Ghats orogenic belt, India. Neues Jahrbuch für Mineralogie Abhandlungen 148, 97–112.

Nagasawa, H., 1970. Rare Earth concentrations in zircon and apatite and their host dacite and granites. Earth and Planetary Science Letters 9, 359–364.

Nelson, D.R., McCulloch, M.T., 1989. Enriched mantle components and mantle recycling of sediments. In: Ross, J. (Ed.), Kimberlites and Related Rocks, vol 1. Their Composition, Occurrence, Origin and Emplacement. Geological Society of Australia Special Publication, vol. 14, pp. 560–570.

Pandey, B.K., Gupta, J.N., Sarma, K.J., Sastry, C.A., 1997. Sm–Nd, Pb–Pb and Rb–Sr geochronology and petrogenesis of the mafic dyke swarm of Mahbubnagar, South India: implications for Paleoproterozoic crustal evolution of the Eastern Dharwar Craton. Precambrian Research 84, 181–196.

Paslick, C.R., Halliday, A.N., Davies, G.R., Mezger, K., Upton, B.G. J., 1993. Timing of Proterozoic magmatism in the Gardar Province, southern Greenland. Geological Society of America Bulletin 105, 272–278.

Paster, T.P., Schauwecker, D.S., Haskin, L.A., 1974. The behavior of some trace elements during solidification of the Skaergaard layered series. Geochimica et Cosmochimica Acta 38, 1549–1577.

Platt, R.G., 1996. Nepheline syenite complexes—an overview. In: Mitchell, R.H. (Ed.), Undersaturated Alkaline Rocks: Mineralogy, Petrogenesis, and Economic Potential. Mineralogical Association of Canada, Short Course Volume, vol. 24, pp. 63–99.

Price, R.C., Johnson, R.W., Gray, C.M., Frey, F.A., 1985. Geochemistry of phonolites and trachytes from the summit region of Mount Kenya. Contributions to Mineralogy and Petrology 89, 394–409.

Prowatke, S., Klemme, S., 2005. Effect of melt composition on the partitioning of trace elements between titanite and silicate melts. Geochimica et Cosmochimica Acta 69, 695–709.

Rao, A.D.P., Rao, K.N., Murthy, Y.G.K., 1987. Gabbro–anorthosite–pyroxenite complexes and alkaline rocks of Chimakurti–Elchuru area, Prakasam District, Andhra Pradesh. Reconnaissance Geological Survey of India 116, 1–20.

Ratnakar, J., Vijaya Kumar, K., 1995. Petrogenesis of quartz-bearing syenite occurring within nepheline syenite of the Elchuru Alkaline Complex, Prakasam Province, Andhra Pradesh. Journal of the Geological Society of India 46, 611–618.

Rehkämper, M., Hofmann, A.W., 1997. Recycled ocean crust and sediment in Indian Ocean MORB. Earth and Planetary Science Letters 147, 93–106.

Rickers, K., Mezger, K., Raith, M.M., 2001. Evolution of the continental crust in the Proterozoic Eastern Ghats Belt, India and new constraints for Rodinia reconstruction: implications from Sm–Nd, Rb–Sr and Pb–Pb isotopes. Precambrian Research 112, 183–210.

Rogers, N.W., Hawkesworth, C.J., Parker, R.J., Marsh, J.S., 1985. The geochemistry of potassic lavas from Vulsini, central Italy and implications for mantle enrichment processes beneath the Roman region. Contributions to Mineralogy and Petrology 90, 244–257.

Sarkar, A., Paul, D.K., 1998. Geochronology of the Eastern Ghats Precambrian mobile belt—a review. Geological Survey of India Special Publication 44, 51–86.

Schreurs, J., 1985. Prograde metamorphism of metapelites, garnet–biotite thermometry and prograde changes of biotite chemistry in high grade rocks of West Uusimaa, southwest Finland. Lithos 18, 69–80.

Sheraton, J.W., England, R.N., 1980. Highly potassic mafic dykes from Antarctica. Journal of the Geological Society of Australia 27, 129–135.

Simmat, R., 2003. Identifizierung hochgradig metamorpher Provinzen des Eastern Ghats Belt in Indien anhand einer EMS-Studie von Monazit-Altersmustern. Unpublished Ph.D. thesis, University of Bonn, Germany.

Simmons, E.C., Hedge, C.E., 1978. Minor-element and Sr-isotope geochemistry of Tertiary stocks, Colorado mineral belt. Contributions to Mineralogy and Petrology 67, 379–396.

Singh, A.P., Mishra, D.C., 2002. Tectonosedimentary evolution of Cuddapah basin and Eastern Ghats Mobile Belt (India) as Proterozoic collision: gravity, seismic and geodynamic constraints. Journal of Geodynamics 33, 249–267.

Stacey, J.S., Kramers, J.D., 1975. Approximation of terrestrial lead isotope evolution by a two stage model. Earth and Planetary Science Letters 26, 207–221.

Subba Rao, T.V., Bhaskar Rao, Y.J., Siva Raman, T.V., Gopalan, K., 1989. Rb–Sr age and petrology of the Elchuru alkaline complex: implications to alkaline magmatism in the Eastern Ghats Mobile Belt. Memoirs Geological Society of India 15, 207–223.

Tatsumoto, M., Knight, R.J., Allègre, C.J., 1973. Time differences in the formation of meteorites as determined from the ratio of lead-207 to lead-206. Science 180, 1279–1283.

Taylor, S.R., McLennan, S.M., 1985. The Continental Crust: Its Composition and Evolution. Blackwell, Oxford.

Thornton, C.P., Tuttle, O.F., 1969. Chemistry of igneous rocks: I. Differentiation Index. American Journal of Science 258, 664–684.

Upadhyay, D., Raith, M.M., in press. Intrusion age, geochemistry and metamorphic conditions of a quartz-monzonite intrusion at the craton–Eastern Ghats Belt suture near Jojuru, India. Gondwana Research.

Upadhyay, D., Raith, M.M., Mezger, K., Bhattacharya, A., Kinny, P. D., in press. Mesoproterozoic rifting and Pan-African continental collision in South-Eastern India: evidence from the Khariar alkaline complex. Contributions to Mineralogy and Petrology.

Upadyhyay, D., Raith, M.M., submitted for publication. Petrogenesis of the Kunavaram alkaline complex: implications for the evolution of the craton-Eastern Ghats Belt suture, SE India. Precambrian Research.

Upton, B.G.J., 1987. Gabbroic, syenogabbroic and syenitic cumulates of the Tugtutoq Younger Giant Dyke Complex, South Greenland. In: Parsons, I. (Ed.), Origins of Igneous Layering. Reidel, Dordrecht-Boston, NATO ASI Series, Series C: Mathematical and Physical Sciences, vol. 196, pp. 93–123.

Upton, B.G.J., Emeleus, C.H., 1987. Mid-Proterozoic alkaline magmatism in southern Greenland; the Gardar Province. In: Fitton, J.G., Upton, B.G.J. (Eds.), Alkaline Igneous Rocks. Geological Society Special Publication, vol. 30, pp. 449–471.

Vasudevan, D., Kröner, A., Wendt, I., Tobschall, H., in press. Geochemistry, petrogenesis and age of felsic to intermediate metavolcanic rocks from the Paleoproterozoic Nellore Schist Belt, Vinjamur, Andhra Pradesh, India. Journal of Asian Earth Sciences.

Vijaya Kumar, K., Ratnakar, J., 1995. The gabbros of Prakasam alkaline province, Andhra Pradesh, India. Journal of the Geological Society of India 46, 245–254.

Villemant, B., Jaffrezic, H., Joron, J.L., Treuil, M., 1981. Distribution coefficients of major and trace-elements—fractional crystallization in the alkali basalt series of Chaîne-des-Puys (Massif Central, France). Geochimica et Cosmochimica Acta 45, 1997–2016.

Vinogradov, A.P., Turgarino, A.I., Zhjkov, C., Stapnikova, N., Bibikova, E., Khores, K., 1964. Geochronology of Indian Precambrian. 10th Int. Geol. Congr. New Delhi, pp. 553–567.

Wasserburg, G.J., Jacobsen, S.B., DePaolo, D.J., McCulloh, M.T., Wen, J., 1981. Precise determinations of Sm/Nd ratios, Sm and Nd isotopic abundances in standard solutions. Geochimica et Cosmochimica Acta 45, 2311–2323.

Watson, E.B., Green, T.H., 1981. Apatite/liquid partition coefficients for the rare earth elements and strontium. Earth and Planetary Science Letters 56, 405–421.

Wetherill, G.W., 1956. Discordant uranium–lead ages. Trans American Geophysical Union 37, 320–326.

Weyer, S., Münker, C., Rehkämper, M., Mezger, K., 2002. Determination of ultra-low Nb, Ta, Zr and Hf concentrations and the chondritic Zr/Hf and Nb/Ta ratios by isotope dilution analyses with multiple collector ICP-MS. Chemical Geology 187, 295–313.

Weyer, S., Münker, C., Mezger, K., 2003. Nb/Ta, Zr/Hf and REE in the depleted mantle: implications for the differentiation history of the crust–mantle system. Earth and Planetary Science Letters 205, 309–324.

Williams, I.S., 1998. U–Th–Pb geochronology by ion microprobe. In: McKibben, M.A., Shanks III, W.C., Ridley, W.I. (Eds.), Applications of micro analytical techniques to understanding mineralizing processes. Reviews in Economic Geology, vol. 7, pp. 1–35.

Woolley, A.R., Platt, R.G., 1986. The mineralogy of nepheline syenite complexes from the northern part of the Chilwa Province, Malawi. Mineralogical Magazine 50, 597–610.

Woolley, A.R., Platt, R.G., Nelson Eby, G., 1996. Relatively aluminous alkali pyroxene in nepheline syenites from Malawi: mineralogical response to metamorphism in alkaline rocks. Canadian Mineralogist 34, 423–434.

Zhao, J.X., Shiraishi, K., Ellis, D.J., Sheraton, J.W., 1995. Geochemical and isotopic studies of syenites from the Yamato Mountains, East Antarctica: implications for the origin of syenite magmas. Geochimica et Cosmochimica Acta 59, 1363–1382.

Zhao, G., Sun, M., Wilde, S.A., Li, S., 2004. A Paleo-Mesoproterozoic supercontinent: assembly, growth and breakup. Earth-Science Reviews 67, 91–123.

Zindler, A., Hart, S.R., 1986. Chemical geodynamics. Annual Review Earth and Planetary Sciences 14, 493–571.

Zuleger, E., Erzinger, J., 1988. Determination of the REE and Y in silicate materials with ICP-AES. Fresenius Zeitschrift für Analytische Chemie 332, 140–143.